ENVISAT GOMOS Monthly report: March 2006

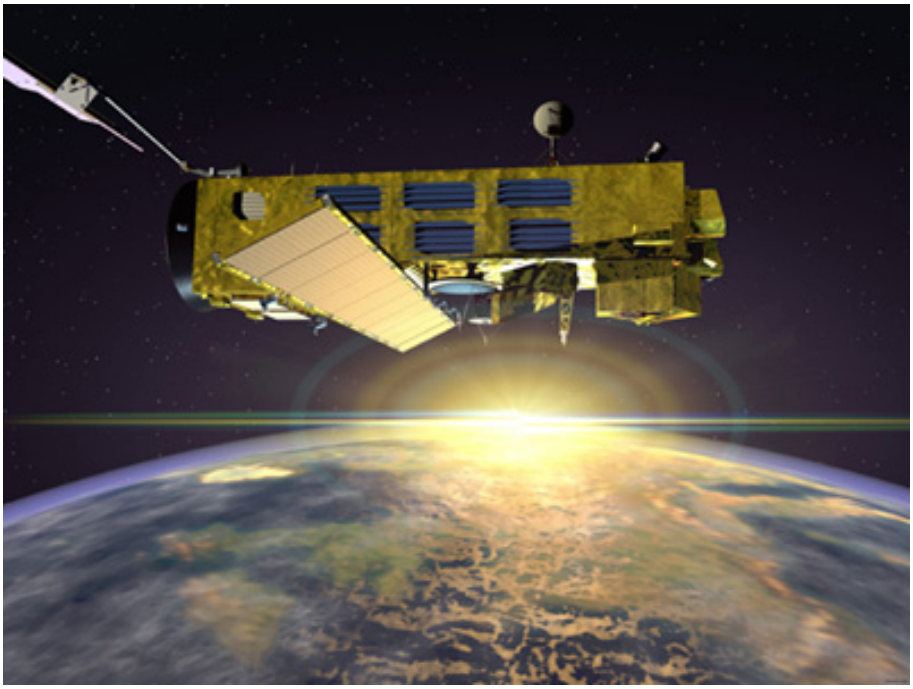

Prepared by:	Lidia Saavedra de Miguel – SERCO
Checked by:	Sian Procter – VEGA
Approved by:	Gilbert Barrot – ACRI
Inputs from:	GOMOS Quality Working Group, ECMWF

Issue:	1.0
Reference:	ENVI-SPPA-EOPG-TN-06-0014
Date of issue:	12th April 2006
Status:	Reviewed
Document type:	Technical Note

TABLE OF CONTENTS

1 INTRODUCTION

The GOMOS monthly report documents the current status and recent changes to the GOMOS instrument, its data processing chain, and its data products.
The Monthly Report (hereafter MR) is composed of analysis results obtained by the Data Processing and Quality Control, combined with inputs received from the different entities working on GOMOS operation, calibration, product validation and data quality. These teams participate in the GOMOS Quality Working Group:

- European Space Agency (ESRIN, ESOC, ESTEC-PLSO)
- DPQC
- ACRI
- Service d'Aeronomie
- Finnish Meteorological Institute
- IASB-Belgian Institute for Space Aeronomy
- Astrium Space
- ECMWF

In addition, the group interfaces with the Atmospheric Chemistry Validation Team.

1.1 Scope

The main objective of the Monthly Report is to give, on a regular basis, the status of GOMOS instrument performance, data acquisition, results of anomaly investigations, calibration activities and validation campaigns. The following six sections compose the MR:

- Summary
- Unavailability
- Instrument Configuration and Performance
- Level 1 Product Quality Monitoring
- Level 2 Product Quality Monitoring
- Validation Activities and Results

1.2 References

[1] ENVISAT Weekly Mission Operations Report #193, 194#, #195, #196 ENVI-ESOC-OPS-RP-1011-TOS-OF
[2] ECMWF GOMOS Monthly Reports

1.3 Acronyms and Abbreviations

ACVT Atmospheric Chemistry Validation Team
ADC Analogue-to-Digital Converter

ADF	Auxiliary Data File
ADS	Auxiliary Data Server
ANX	Ascending Node Crossing
ARB	Anomaly Review Board
ARF	Archiving Facility (PDS)
CCU	Central Communication Unit
CFS	CCU Flight Software
CNES	Centre National d'Études Spatiales
CTI	Configuration Table Interface / Configurable Transfer Item
CR	Cyclic Report
DC	Dark Charge
DMOP	Detailed Mission Operation Plan
DPM	Detailed Processing Model
DPQC	Data Processing and Quality Control
DS	Data Server
DSA	Dark Sky Area
DSD	Data Set Descriptor
ECMWF	European Centre for Medium Weather Forecast
EQSOL	Equipment Switch Off Line
ESA	European Space Agency
ESL	Expert Support Laboratory
ESRIN	European Space Research Institute
ESTEC	European Space Research & Technology Centre
ESOC	European Space Operations Centre
FCM	Fine Control Mode
FMI	Finnish Meteorological Institute
FOCC	Flight Operations Control Centre (ENVISAT)
FP1	Fast Photometer 1
FP2	Fast Photometer 2
GADS	Global Annotations Data Set
GOMOS	Global Ozone Monitoring by Occultation of Stars
GOPR	Gomos Prototype
GS	Ground Segment
HK	Housekeeping
IASB	Institut d'Aeronomie Spatiale de Belgique
IAT	Interactive Analysis Tool
ICU	Instrument Control Unit
IDL	Interactive Data Language
IECF	Instrument Engineering and Calibration Facilities
IMK	Institute of Meteorology Karlsruhe (Meteorologisch Institut Karlsuhe)
INV	Inventory Facilities (PDS)
IPF	Instrument Processing Facilities (PDS)
JPL	Jet Propulsion Laboratory
LAN	Local Area Network
LMA	Levenberg-Marquardt Algorithm
LPCE	Laboratoire de Physique et Chimie de l'Environnement
LUT	Look Up Table
MCMD	Macro Command

MDE	Mechanism Drive Electronics
MIP	Most Illuminated Pixel
MPH	Main Product Header
MPS	Mission Planning System
MR	Monthly Report
OBT	On Board Time
OCM	Orbit Control Manoeuvre
OOP	Out-of-plane
OP	Operational Phase of ENVISAT
PAC	Processing and Archiving Centre (PDS)
PCF	Product Control Facility
PDCC	Payload Data Control Centre (PDS)
PDHS	Payload Data Handling Station (PDS)
PDHS-E	Payload Data Handling Station – ESRIN
PDHS-K	Payload Data Handling Station – Kiruna
PDS	Payload Data Segment
PEB	Payload Equipment Bay
PLSOL	Payload Switch off Line
PMC	Payload Module Computer
PRNU	Pixel Response Non Uniformity
PSO	On-Orbit Position
QC	Quality Control
QUARC	Quality Analysis and Reporting Computer
QWG	Quality Working Group
RGT	ROP Generation Tool
RIVM	Rijksinstituut voor Volksgezondheid en Milieu
ROP	Reference Operations Plan
RTS	Random Telegraphic Signal
SA	Service d'Aeronomie
SAA	South Atlantic Anomaly
SATU	Star Acquisition and Tracking Unit
SFA	Steering Front Assembly
SFCM	Stellar Fine Control Mode
SFM	Steering Front Mechanism
SMNA	Servicio Meteorológico Nacional de Argentina
SODAP	Switch On and Data Acquisition Phase
SPA1	Spectrometer A CCD 1
SPA2	Spectrometer A CCD 2
SPB1	Spectrometer B CCD 1
SPB2	Spectrometer B CCD 2
SPH	Specific Product Header
SQADS	Summary Quality Annotation Data Set
SSP	Sun Shade Position
SZA	Solar Zenith Angle
VCCS	Voice Coil Command Saturation

2 SUMMARY

Operations (section 4.1.2):

- On 12th March the reduced azimuth window was moved from [-5°, +20°] to [+10°, +35°] in order to support the SAUNA validation campaign
- On 14th March ESOC had to remove 2 orbits from the GOMOS planning due to a problem in the macro-command scheduling. Therefore no data were generated from 03:01 to 06:22
- Between 27th March 02:43 and 28th March 13:08 GOMOS operations had to be interrupted due to the ENVISAT OCM manoeuvre. Because of the OCM, the GOMOS SFM should be parked to the Sun Shade Position and it was performed with the nominal procedure 24 hours before the manoeuvre. On 27th March 02:43:34 a Voice coil anomaly occurred and the anomaly "SSP not reached" was reported. Due to this anomaly GOMOS went into Standby/refuse mode. The recovery was performed soon but lots of Voice coil anomalies occurred and the following commanded transition to Sun Shade Position failed. At this point the mirror is very close to the SSP and it was considered safe for the OCM. Following the manoeuvre the measurement started (28th March 13:08) and GOMOS suffered many occurrences of "Voice coil command saturation current" anomaly which caused 49 stars to be lost. On 28th March at 16:50 the instrument resumed operations nominally.

Data availability (when instrument was in operation): For March the level 0 data availability is around 99.5% while for level 1b the archived products are around 78%. The reason for the low statistics on level 1b products is that the allocated processing time is lower than the real processing time with the result that the end of the orbit is systematically not processed. Now the problem is known and should be solved (section 3.4).

Temperatures: The CCD temperatures show the expected global increase due to the radiator ageing. Another expected variation of the temperatures, the seasonal one, with amplitude of around 0.8 degree can also be observed (section 4.3).

Modulation signal: The standard deviation of the modulation signal presents high values during summer time. The South Atlantic Anomaly is now confirmed as the cause of these unexpected peaks. The quality of ESRIN data, in particular over the SAA zone, is impacted but the measure of this impact is under investigation. However, in the second half of October, the peaks are smaller because the DSA zone where the data are taken for this analysis is moving towards the Northern Hemisphere. At the end of October the DSA zone is definitely chosen by the planning system in the Northern Hemisphere (to fill the criteria 'DSA in full dark limb conditions') and the high peaks disappear (section 4.5.2).

Star detection performance: the stars should be detected not far from the SATU center, that is, pixel number 145 in elevation and number 205 in azimuth. It has been observed that the azimuth MIP was within the threshold since September 2002 until the occurrence of the VCCS anomaly on January 2005. The reason for the change in trend observed after the anomaly is, at the moment, not understood. The elevation MIP had a significant variation until 12th December 2003 when a new PSO algorithm was activated in order to reduce the deviations of the ENVISAT platform attitude with respect to the nominal one. Similarly to the azimuth, after the anomaly of January 2005 the Elevation MIP has a drift that has no explanation. Investigations are ongoing to try to understand this behavior of the MIP as although it does not impact the data quality, it may invalidate attitude monitoring by GOMOS and could represent a hidden anomaly (section 4.6.3).

Pointing performance: the SATU NEA had a sudden increase on 8th September 2005 mainly in 'Y' axis. These values remained high, fluctuating between 1 and 1.8 microrad until December 2005 when they came back to the values they used to be before the increase of September. The cause of this unexpected behavior is under investigation although the values were always below the threshold (section 4.6.1).

Radiometric sensitivity monitoring: for stars 25 and 9, the UV ratio is greater than the threshold 10%. It is clear that there is a global decrease of UV ratios for all the stars. This confirms the expected degradation suffered by the UV optics that is, anyway, very small considering also the small variation for the rest of the stars. For the photometers radiometric sensitivity ratios it is observed that every star has a variation that seems to be seasonally related. The variation is significant for stars 25 and 18. After some investigations performed by the QWG, it has been concluded that the problem is not linked to the photometers. A further indication that the problem is not on the photometer sensitivity is that every star has a very different behaviour (section 5.4.1).

Dark Charge calibration: new calibration ADF's (GOM_CAL_AX files) were disseminated during the reporting period with updated DC calibration maps (see dates and orbits used for the calibrations in section 5.1.2).

3 INSTRUMENT UNAVAILABILITY

3.1 GOMOS Unavailability Periods

In table 3.1-1 there is a list of GOMOS unavailability reports issued during the period 1st to 31st March 2006. Between 27th March 02:43 and 28th March 13:08 GOMOS operations had to be interrupted due to the ENVISAT OCM manoeuvre. Because of the OCM, the GOMOS SFM should be parked to the Sun Shade Position and it was performed with the nominal procedure 24 hours before the manoeuvre. On 27th March 02:43:34 a Voice coil anomaly occurred and the anomaly "SSP not reached" was reported. Due to this anomaly GOMOS went into Standby/refuse mode. The recovery was performed soon but lots of Voice coil anomalies occurred and the following commanded transition to Sun Shade Position failed. At this point the mirror is very close to the SSP and it was considered safe for the OCM. Following the manoeuvre the measurement started and GOMOS suffered many occurrences of "Voice coil command saturation current" anomaly which caused 49 stars to be lost. On 28th March at 16:50 the instrument resumed operations nominally.

Table 3.1-1: List of unavailability periods issued during the reporting period

Reference of unavailability report	Start time Star orbit	Stop time Stop orbit	Description
EN-UNA-2006/0104	27 Mar 2006 02:43:00 Orbit 21285	28 Mar 2006 13:08:16 Orbit = 21306	Configured for scheduled OCM. Switch to Standby/Refuse due to known anomaly: SSP not reached due to VCCS anomaly

3.2 Stars Lost in Centering

The acquisition of a star initiates with a rallying phase where the telescope mechanism is directed towards the expected position of the star. Subsequently the acquisition procedure enters into detection mode, where the SATU star tracker output signal is pre-processed for spot presence survey and for the location of the most illuminated couple of adjacent pixels for two added lines, over the detection field. The Most Illuminated Pixel (MIP) defines the position of the first SATU centering window. The following step in the acquisition sequence is then initiated and consists of a centering phase where the SATU output signal is pre-processed for spot presence survey over the maximum of 10x10 pixel field. This allows the third phase to begin: the tracking phase.

The centering phase has occasionally resulted in loss of the star from the field of view. Fig. 3.2-1 reports the percentage of the stars lost in centering for the period 03-FEB-2003 to 26-MAR-2006. It can be seen that three stars, mainly weak stars (higher star id means higher magnitude) are lost during the centering phase between 4 and 6 % of their planned observations. The star id 115 was lost 40% of the times but it was planned to be occulted five times and was lost twice (in period 19-25 January 2004), so this high percentage of loss is not statistically significant.

As the monitoring shows neither a trend nor excessively high percentages of loss, there is no need for the moment to reject any star from the catalogue, and there is no indication of instrument-related problems.

Now with the instrument in a new operation scenario, the stars are also lost due to the anomaly “elevation voice coil command saturation” even if the instrument is not going anymore to Stand by / Refuse mode (section 3.3).

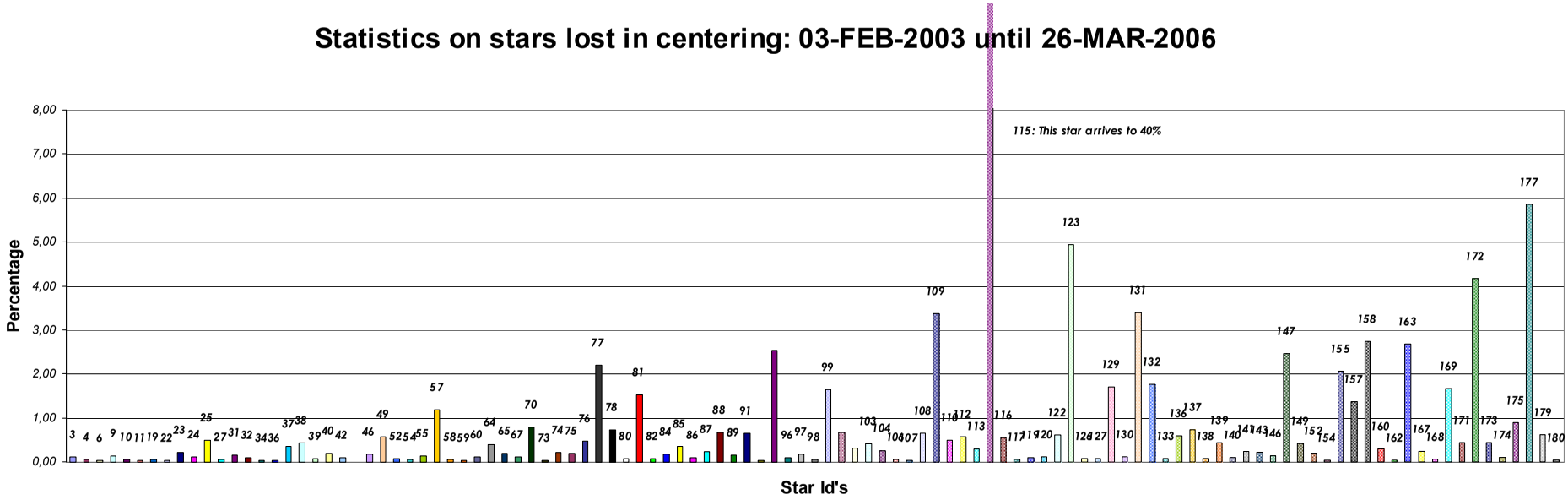

Figure 3.2-1: Statistics on stars that have been lost during the centering phase. The number above the columns correspond to the Star ID

3.3 Stars lost due to VCCS anomaly

VCCS anomalies occurred when moving the mirror to the sun shade position prior to the manoeuvre on 27th March 2006. At the moment of restarting the measurement after the manoeuvre on 28th March, the VCCS occur again with the subsequent lost of 49 stars.

3.4 Data Generation Gaps

The trend in percentage of available data within the archives PDHS-K and PDHS-E is depicted in fig. 3.4-1 (when instrument was in operation). It is a good indicator on how the PDS chain is working in terms of generation and dissemination of data to the archives. The percentage is calculated once per week.

For March the level 0 data availability is around 99.5% while for level 1b the archived products are around 78%. The reason for the low statistics on level 1b products is that the allocated processing time is lower than the real processing time with the result that the end of the orbit is systematically not processed. Now the problem is known and should be solved.

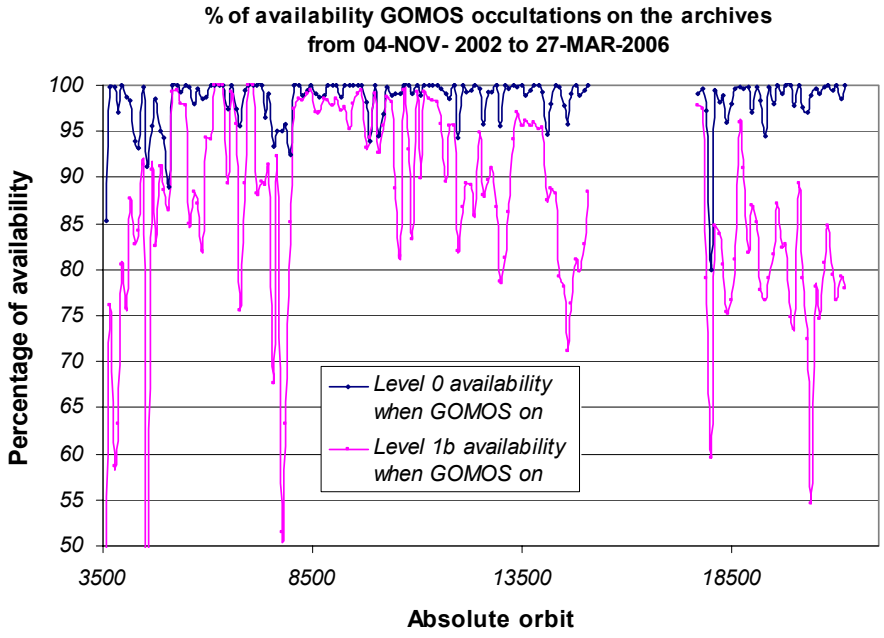

Figure 3.4-1: Percentage of level 0 and level 1b data availability on the archives PDHS-E and PDHS-K

3.4.1 LEVEL 0 PRODUCTS: GOM_NL__0P

Occultations planned to be acquired but for which no GOM_NL__0P data product has become available are presented in fig. 3.4-2 for the reporting period.

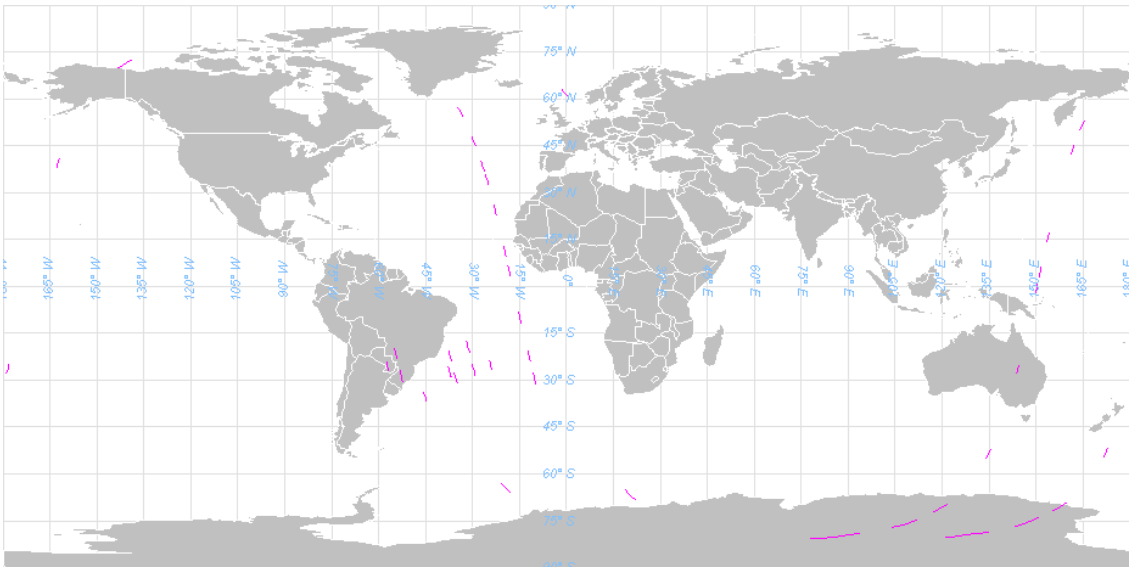

Figure 3.4-2: The pink lines are the orbit segments corresponding to planned data acquisitions for which no GOMOS level 0 product has become available

3.4.2 HIGHER LEVEL PRODUCTS

Routine dissemination of higher-level products produced by the PDS to the users is enabled. Reprocessed products (level 2) are available at D-PAC ftp server ftp-ops.de.envisat.esa.int from August 2002 to December 2005. Existing holes will be covered by new products generated early in 2006. The next operational processor (the current version is GOMOS 4.02, the next one will be GOMOS/5.00) that generates data in near real time will be in line with the prototype used for the reprocessing.

4 INSTRUMENT CONFIGURATION AND PERFORMANCE

4.1 Instrument Operation and Configuration

4.1.1 HISTORIC OPERATIONS

During the period end of March 2003 to July 2003 the azimuth range had to be decreased in steps (table 4.1-1) to avoid an instrument problem ("Voice_coil_command_saturation" anomaly) that caused GOMOS to go into STAND BY/REFUSE mode. On July 2003 the driver assembly was switched to the redundant B-side and since that date the full azimuth range (-10.8, +90.8) was again available until the second major anomaly occurred on 25th January 2005. Between this date and until the instrument was declared operational again (29th August 2005), GOMOS has been operated for testing and anomaly investigation purposes in different operations scenarios. The historical changes in azimuth configuration are summarized in table 4.1-1.

Table 4.1-1: Historical changes in Azimuth configuration when GOMOS is operational

Date	Orbit	Minimum Azimuth (°)	Maximum Azimuth (°)
29-MAR-2003 17:40	5635	0.0	+90.8
31-MAY-2003 06:22	6530	+4.0	+90.8
16-JUN-2003 16:17	6765	+12.0	+90.8
15-JUL-2003 01:39	7200	-10.8	+90.8
25-JAN-2005 23:33	15200	tests	tests
29-AUG-2005 02:52	18280	-10	+10
26-SEP-2005 01:32	18680	-5	+20
03-OCT-2005 01:12	18780	-5	+15
09-OCT-2005 21:30	18878	-5	+20
12-MAR-2006 17:29	21080	+10	+35

4.1.2 CURRENT OPERATIONS AND CONFIGURATION

The planned GOMOS operations for the reporting period are identified in table 4.1-2. Due to a problem in the macro-command scheduling, ESOC had to remove 2 orbits from the GOMOS planning. Therefore no data were generated from 03:01 to 06:22 of 14th March.

The operation scenario of GOMOS since 29th August 2005 until end of reporting month consists of:

- Planning 2 orbits per sequence (nominal were 5): this is done because in case of a voice coil failure with subsequent loss of star observation, the maximum loss of consecutive observations cannot exceed two orbits.
- Reduced azimuth field of view (nominal was [-10°, +90°]): as the anomaly occurs during the rallying of the telescope in the preparation for the star observation, it has been decided to reduce the field of view in order to minimize the failure occurrence probability. On 12th March 2006 the reduced azimuth window was moved from [-5°, +20°] to [+10°, +35°] in order to support the SAUNA validation campaign.

Table 4.1-2: GOMOS planned operations. The planning is built on a 2-orbit sequence basis (2 orbits with the same stars)

UTC Start	Start Orbit	Stop Orbit	Mode (Asynchronous or Synchronous)	Calibration (CAL) Dark Sky Area (DSA) or Nominal (Nom)
01-MAR-2006 03:09:54	20914	21179	S	Nom
19-MAR-2006 17:09:11	21180	21187	A	CAL75
20-MAR-2006 06:33:59	21188	21355	S	Nom

There was no new Configurable Table Interface (CTI) uploaded to the instrument. The files used since the beginning of the mission are in table 4.1-3.

Table 4.1-3: Historic CTI Tables

CTI filename	Dissemination to FOCC
CTI_SMP_GMVIEC20030716_123904_00000000_00000004_20030715_000000_20781231_235959.N1	16-JUL-2003
CTI_SMP_GMVIEC20021104_075734_00000000_00000003_20021002_000000_20781231_235959.N1	06-NOV-2003
CTI_SMP_GMVIEC20021002_082339_00000000_00000002_20021002_000000_20781231_235959.N1	07-OCT-2003
CTI_SMP_GMVIEC20020207_154455_00000000_00000000_20020301_032709_20781231_235959.N1	21-FEB-2002

4.2 Limb, Illumination conditions and instrument gain setting

The **limb** and the **illumination condition** are two parameters that can confuse the user community. In table 4.2-1 there are specified the product parameter (level 1b and level 2 of operational processor GOMOS/4.02) where the flag is located, the meaning and the source. The difference between the limb (SPH/bright_limb) and the illumination condition (SUMMARY_QUALITY/limb_flag) is that the first one is coming from the mission scenario and the second is coming from the processing (defined from the computation of the sun zenith and azimuth angles at both instrument and tangent point locations). The SPH/bright_limb is for some occultations set to "dark" in the mission scenario while they are in fact in bright limb illumination conditions. To select the highest quality data for scientific applications, data with SUMMARY_QUALITY/limb_flag equal to '0' should be used (see also the disclaimer: http://envisat.esa.int/dataproducts/availability/disclaimers). The instrument gain settings are also specified in table 4.2-1 (they depend on the mission scenario flags) just for completeness of information.

Table 4.2-1: Relationship between limb, illumination condition flags and instrument gain settings (operational IPF version GOMOS/4.02)

Products parameter	SPH/bright_limb	0 = Dark	1 = Bright	Coming from mission scenario
	SUMMARY_QUALITY/limb_flag	0 = Full Dark 1 = Bright 2 = Twilight	1 = Bright 2 = Twilight	In the geolocation process the sun zenith angle is computed and the occultation then is flagged accordingly
Instrument Gain	SPA Gain	3 (2)	0	Gain setting for spectrometer A. In parenthesis, values valid only for Sirius occultations (starID=1)
	SPB Gain	0	0	Gain setting for spectrometer B

The same is valid for the prototype version GOPR_6.0a_6.0a and following ones (including the one that is used for the on-going second reprocessing of 2002-2005 years), where the **limb** is in fields SPH/bright_limb and SUMMARY_QUALITY/dark_bright_limb and the **illumination condition** is in field SUMMARY_QUALITY/obs_ill_cond. For these prototypes, the illumination condition can have five values (see table 4.2-2).

Table 4.2-2: Relationship between limb, illumination condition flags and instrument gain settings (prototype version GOPR 6.0a_6.0a and following ones)

Products parameter	SPH/bright_limb SUMMARY_QUALITY/dark_bright_limb	0 = Dark	1 = Bright	Coming from mission scenario
	SUMMARY_QUALITY/obs_ill_cond	0 = Full Dark 1 = Bright 2 = Twilight 3 = Straylight 4 = Twi.+Stray.		In the geolocation process the sun zenith angle is computed and the occultation is then flagged accordingly
Instrument Gain	SPA Gain	3 (2)	0	Gain setting for spectrometer A. In parenthesis, values valid only for Sirius occultations (starID=1)
	SPB Gain	0	0	Gain setting for spectrometer B

4.3 Thermal Performance

Since the beginning of the mission, the hot pixel and RTS phenomena have been producing a continuous increase of the dark charge signal within the CCD detectors (see section 4.5.1). In order to minimize this effect, three successive CCD cool downs were performed in orbits 800 (25th April 2002), 1050 (13th May 2002) and 2780 (11th September 2002) with a total decrease in temperature of 14 degrees.

Fig. 4.3-1 and 4.3-2 display, respectively, the overall temperature variation and the temperature variation around the Ascending Node Crossing (ANX) time with a resolution of 0.4 degrees (coding accuracy for level 0 data). The CCD temperatures show the expected global increase due to the radiator ageing.

Another expected variation of the temperatures, the seasonal one, with amplitude of around 0.8 degree, can be also observed. The peaks that occur mainly in spectrometer B1 and B2 are also to be noted. They happen a little before the ANX for some consecutive orbits and every 8-10 days. Their origin is not known, as we did not find any correlation between these peaks and other activities carried out by other ENVISAT instruments. The CCD temperature at almost the same latitude location (fig. 4.3-2) is monitored in order to detect any inter-orbital temperature variation. The abnormal decreases observed sometimes in all detectors are after GOMOS switch off periods, when the instrument did not have enough time to reach the nominal temperature before starting the measurements.

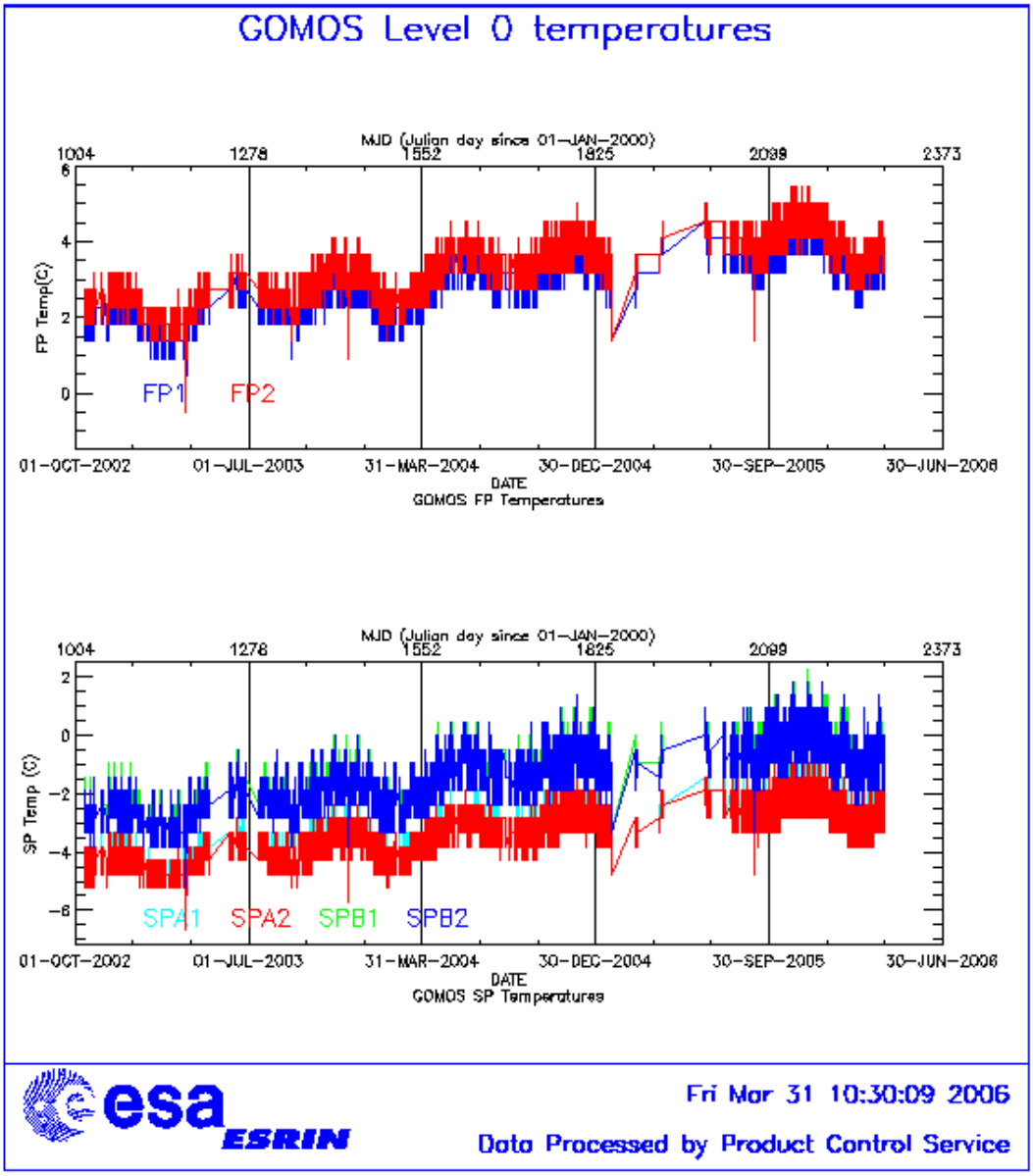

Figure 4.3-1: Level 0 temperature evolution of all GOMOS CCD detectors since October 2002 until the end of the reporting period

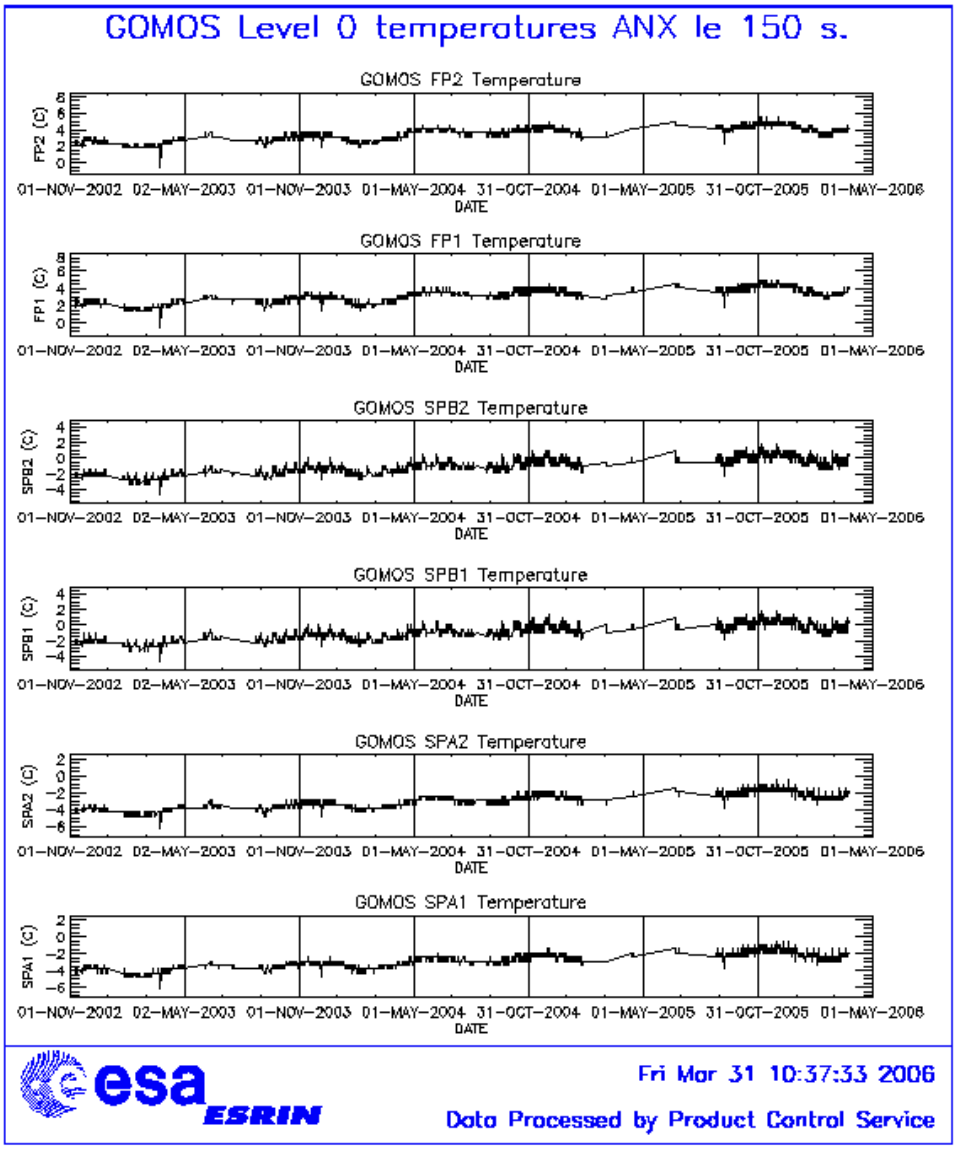

Figure 4.3-2: Level 0 temperature evolution of all GOMOS CCD detectors around ANX since November 2002 until the end of the reporting period

During March 2006, the orbital temperature variation of the detector SPB2 for ascending and descending passes (fig. 4.3-3 and 4.3-4) is nominal, around 3 degrees. The stability of the temperature during the orbit is important because it affects the position of the interference patterns. The phenomenon of the interference is present mainly in SPB and this Pixel Response Non-Uniformity (PRNU) is corrected during the processing.

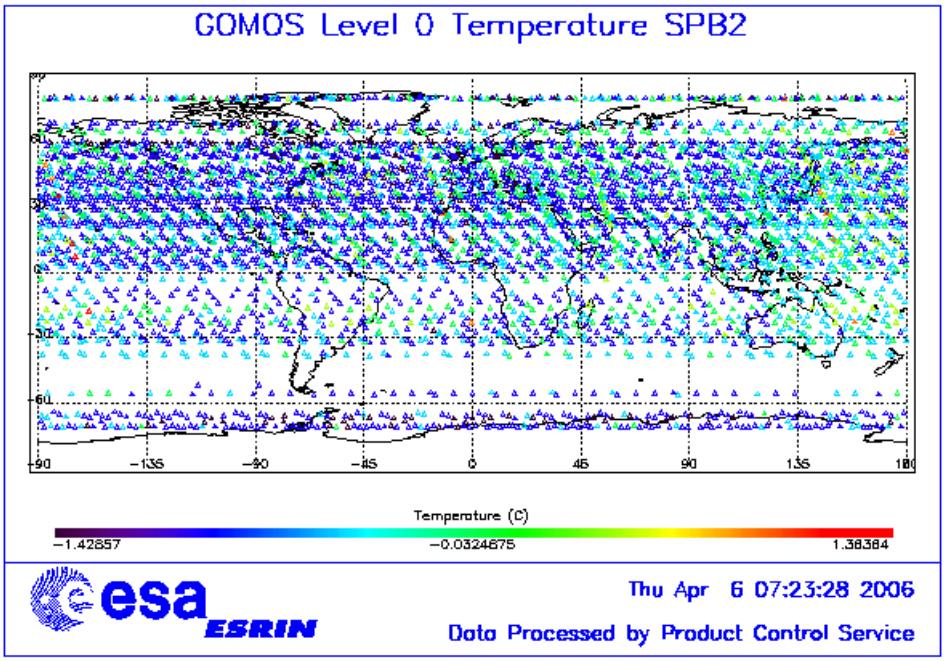

Figure 4.3-3: Ascending orbital variation of SPB2 temperature during reporting period

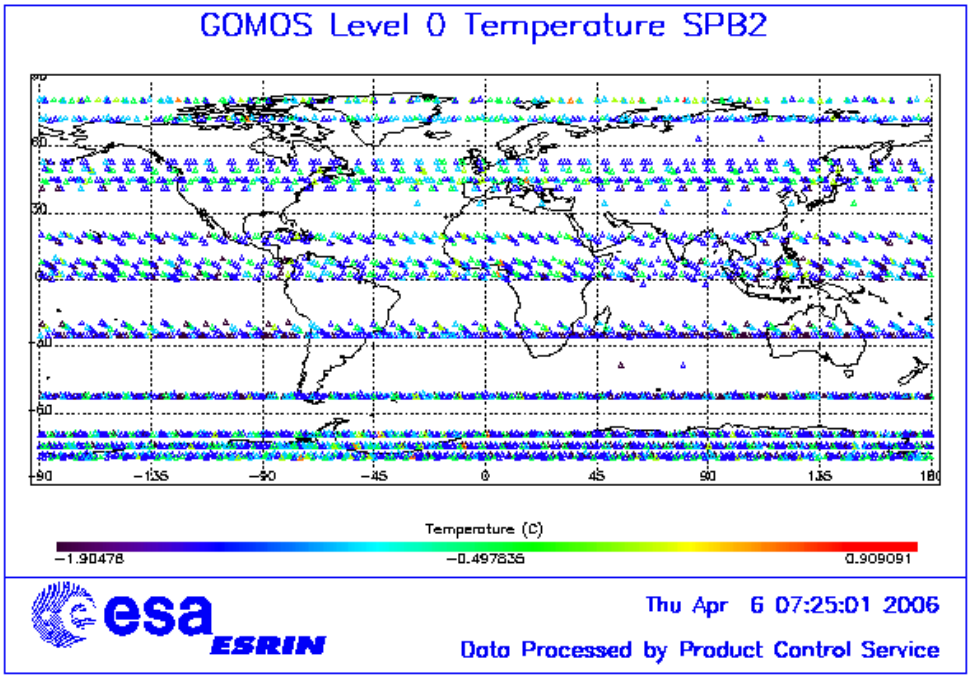

Figure 4.3-4: Descending orbital variation of SPB2 temperature during reporting period

4.4 Optomechanical Performance

No new band setting calibration has been performed during the reporting period. The last one has been done on February 2006.

- Version GOMOS/4.00 and previous ones: in the GOMOS processor versions GOMOS/4.00 and previous, the spectra are expected to be aligned along CCD lines, and therefore use only a single average line index per CCD. In table 4.4-1, the mean values of the location of the star signal for all the calibration analysis done is reported. The 'left' and 'right' values are calculated (the whole interval is not used) because the spectra present a slight slope, more pronounced in spectrometer B (see fig. 4.4-1). In table 4.4-2, mean values of the location of the star signal are calculated for some specific wavelength intervals. These intervals have been changed between the calibration performed in September 2002 and the ones performed afterwards (until November 2003). Table 4.4-3 reports the average location of the star spot on the photometer 1 and 2 CCD.

- Version GOMOS/4.02: in the current processor version (GOMOS/4.02) operational since 23rd March 2004, a Look Up Table (LUT) gives the line index of the spectra location as a function of the wavelength (blue dots in fig. 4.4-1). However this characterization curve is not exactly the location of the star spectrum on the CCD but rather a combination of this position and some artefact created by the shape of the instrument optical point spread function. The exact shape is actually a straight line (especially for SPB) that has been characterised in 2005 and will be implemented in next updates of GOMOS ADF's. In the meantime calibration exercises should be performed in order to check if the LUT values are still valid.

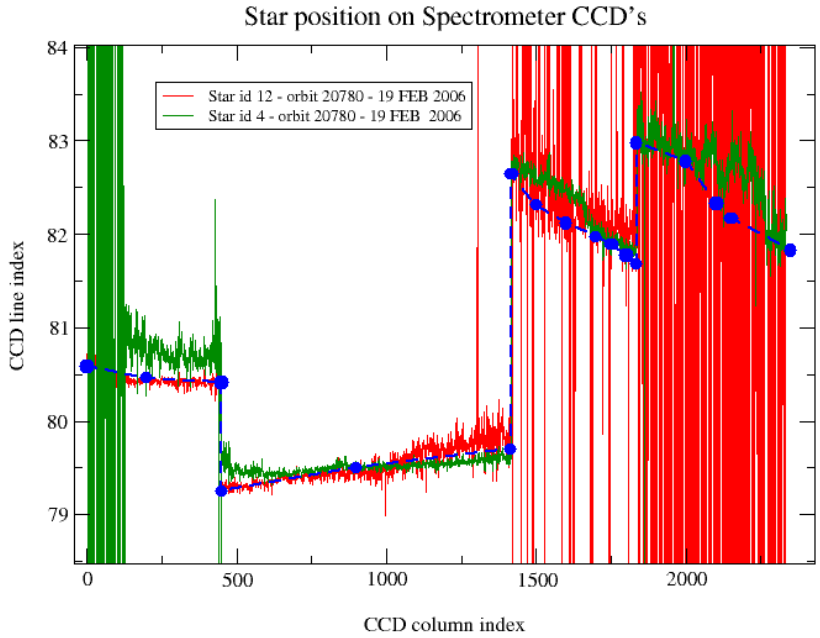

Figure 4.4-1: Average position of star spectra on the CCD

A calibration exercise was performed during February 2006. The position of the stellar spectra of star id 4 and 12 (fig. 4.4-1) observed in dark-limb spatial spread monitoring mode have been averaged above 120 km

altitude and compared to the values of the LUT. The results confirm the LUT values (see table 4.4-4) except for three pixels (in SPB) where a shift is observed. This could be related with the CCD temperatures that are slowly increasing. The need for a recalibration and thus the generation of an updated ADF is not probable due to the imminent arrival of the new GOMOS processor (foreseen to be in operations by the end of April 2006) and its associated set of ADF.

Table 4.4-1: Mean value of the location of the star signal during the occultation at the edges of every band (mean over 50 values, filtering the outliers)

	UV (SPA1) left/right	VIS (SPA2) left/right (Inverted spectra)	IR1 (SPB1) left/right	IR2 (SPB2) left/right
11/09/2002	80.7/80.7	79.8/79.5	82.8/81.9	83.1/82.1
01/01/2003	80.7/80.6	79.8/79.5	82.8/82.0	83.2/82.2
17/07/2003 & 02/08/2003	80.7/80.7	79.8/79.5	82.8/81.9	83.1/82.1
08/11/2003	80.7/80.6	79.8/79.5	82.8/81.9	83.1/82.1

Table 4.4-2: Mean value of the location of the star signal during the occultation (as table 4.4-1) but now within some wavelength intervals

	UV (SPA1)	VIS (SPA2)	IR1 (SPB1)	IR2 (SPB2)
11/09/2002 wl range (nm)	80.8 [300-330]	79.8 [500-530]	82.6 [760-765]	82.9 [937-942]
01/01/2003 wl range (nm)	80.6 [350-360]	78.6 [650-670]	81.6 [760-765]	80.3 [935-945]
02/08/2003	80.6	79.7	82.5	82.8
08/11/2003	80.6	79.9	82.4	82.8

Table 4.4-3: Average column and row pixel location of the star spot on the photometer CCD during the occultation

	FP1 (column/row)	FP2 (column/row)
11/09/2002	11/4	5/5
01/01/2003	10/4	6/4.9
02/08/2003	10/4	6/5
08/11/2003	10/4	6/5

Table 4.4-4: Location of the star signal on the CCD's (corresponding to fig. 4.4-1)

Pixel Column	LUT (Pixel line)	Calibration on 10-APR-2004	Calibration on 04-DEC-2004	Calibration on 27-NOV-2005	Calibration on 19-FEB-2006
0	**80.59**	80.80	80.67	80.93	80.67
20	**80.46**	80.60	80.44	80.32	80.43
449	**80.42**	80.50	80.42	80.40	80.53
450	**79.25**	79.39	79.30	79.16	79.30
900	**79.50**	79.63	79.57	79.36	79.45
1415	**79.70**	79.76	79.76	80.00	79.81
1416	**82.64**	82.80	82.88	82.95	82.76
1500	**82.31**	82.60	82.66	82.63	82.58
1600	**82.12**	82.22	82.30	82.35	82.41
1700	**81.97**	82.04	82.08	82.09	82.05
1750	**81.89**	81.98	82.03	82.00	81.92
1800	**81.78**	81.91	81.96	81.93	81.83
1835	**81.68**	81.88	81.94	81.96	81.79

1836	**82.98**	83.10	83.10	83.27	83.17
2000	**82.78**	82.90	82.94	83.04	82.83
2100	**82.33**	82.70	82.73	82.82	82.83
2150	**82.17**	82.40	82.54	82.79	82.70
2350	**81.83**	82.00	82.00	82.68	81.96

4.5 Electronic Performance

4.5.1 DARK CHARGE EVOLUTION AND TREND

The trend of Dark Charge (DC) is of crucial importance for the final quality of the products, and is therefore subject to intense monitoring. As part of the DC there is:

- "Hot pixels", a pixel is "hot" when its dark charge exceeds its value measured on ground, at the same temperature, by a significant amount.
- RTS phenomenon (Random Telegraphic Signal), it is an abrupt change (positive or negative) of the CCD pixel signal, random in time, affecting only the DC part of the signal and not the photon generated signal.

The temperature dependence of the DC would make this parameter a good indicator of the DC behaviour, but the hot pixels and the RTS are producing a continuous increase of the DC (see trend in fig. 4.5-1 and 4.5-2). To take into account these phenomena, since version GOMOS/4.00 (the current one is GOMOS/4.02) a DC map per orbit is extracted from a Dark Sky Area (DSA) observation performed around ANX (full dark conditions). For every level 1b product (occultation), the actual thermistor temperature of the CCD is used to convert the DC map measured around ANX into an estimate of the DC at the time (and different temperature) of the actual occultation. When the DSA observation is not available, the DC map inside the calibration product that was measured at a given thermistor reference temperature is used; again, the actual thermistor temperature of the CCD is used to compute the actual map. Table 4.5-1 reports the list of products that used the DC maps inside the calibration file due to the non-availability of DSA observation. A "CAL DC map with no T dep." means that, as the temperature information was not available for that occultation, the DC map used is exactly the one inside the Calibration product.

The "quality ranking" of the products depending on DC correction performed is as follows:

- Best quality: products with DC correction using DSA observation inside the orbit
- Less quality than previous ones: products with DC correction using the map inside the calibration product, thermal corrected ('DC map used' in table 4.5-1)
- Less quality than previous ones: products with DC correction using the map inside the calibration product, no thermal corrected ('DC map with no T dep.' in table 4.5-1)

Table 4.5-1: Table of level 1b products that used the Calibration DC maps instead of the DSA observation

Product name	DC information
GOM_TRA_1PNPDE20060302_194047_000000392045_00343_20938_0000.N1	DC map used
GOM_TRA_1PNPDE20060302_194405_000000432045_00343_20938_0001.N1	DC map used
GOM_TRA_1PNPDE20060302_195334_000000482045_00343_20938_0002.N1	DC map used

GOM_TRA_1PNPDE20060302_202132_000000352045_00343_20938_0003.N1	DC map used
GOM_TRA_1PNPDE20060302_202904_000000332045_00343_20938_0004.N1	DC map used
GOM_TRA_1PNPDE20060302_203410_000000352045_00343_20938_0005.N1	DC map used
GOM_TRA_1PNPDE20060302_203544_000000372045_00343_20938_0006.N1	DC map used
GOM_TRA_1PNPDE20060303_204948_000000362045_00358_20953_0000.N1	DC map with no T dep.
GOM_TRA_1PNPDE20060303_205306_000000482045_00358_20953_0001.N1	DC map used
GOM_TRA_1PNPDE20060303_210235_000000472045_00358_20953_0002.N1	DC map used
GOM_TRA_1PNPDE20060303_213031_000000372045_00358_20953_0003.N1	DC map used
GOM_TRA_1PNPDE20060303_213805_000000362045_00358_20953_0004.N1	DC map used
GOM_TRA_1PNPDE20060303_214311_000000342045_00358_20953_0005.N1	DC map used
GOM_TRA_1PNPDE20060303_214444_000000352045_00358_20953_0006.N1	DC map used
GOM_TRA_1PNPDE20060307_042618_000000362045_00405_21000_0000.N1	DC map used
GOM_TRA_1PNPDE20060307_043124_000000352045_00405_21000_0001.N1	DC map used
GOM_TRA_1PNPDE20060307_043258_000000342045_00405_21000_0002.N1	DC map used
GOM_TRA_1PNPDE20060307_043434_000000352045_00405_21000_0003.N1	DC map used
GOM_TRA_1PNPDE20060307_044225_000000412045_00405_21000_0004.N1	DC map used
GOM_TRA_1PNPDE20060307_045427_000000422045_00405_21000_0005.N1	DC map used
GOM_TRA_1PNPDE20060307_050330_000000442045_00406_21001_0006.N1	DC map used
GOM_TRA_1PNPDE20060307_050619_000000412045_00406_21001_0007.N1	DC map used
GOM_TRA_1PNPDE20060307_050833_000000362045_00406_21001_0008.N1	DC map used
GOM_TRA_1PNPDE20060307_051005_000000282045_00406_21001_0009.N1	DC map used
GOM_TRA_1PNPDE20060307_051123_000000382045_00406_21001_0010.N1	DC map used
GOM_TRA_1PNPDE20060308_195259_000000382045_00429_21024_0000.N1	DC map used
GOM_TRA_1PNPDE20060308_200514_000000452045_00429_21024_0001.N1	DC map used
GOM_TRA_1PNPDE20060308_201420_000000372045_00429_21024_0002.N1	DC map used
GOM_TRA_1PNPDE20060308_203302_000000352045_00429_21024_0003.N1	DC map used
GOM_TRA_1PNPDE20060308_204043_000000452045_00429_21024_0004.N1	DC map used
GOM_TRA_1PNPDE20060308_204549_000000352045_00429_21024_0005.N1	DC map used
GOM_TRA_1PNPDE20060309_210201_000000382045_00444_21039_0000.N1	DC map used
GOM_TRA_1PNPDE20060309_211415_000000442045_00444_21039_0001.N1	DC map used
GOM_TRA_1PNPDE20060309_212319_000000352045_00444_21039_0002.N1	DC map used
GOM_TRA_1PNPDE20060309_214201_000000372045_00444_21039_0003.N1	DC map used
GOM_TRA_1PNPDE20060309_214943_000000362045_00444_21039_0004.N1	DC map used
GOM_TRA_1PNPDE20060309_215449_000000342045_00444_21039_0005.N1	DC map used
GOM_TRA_1PNPDE20060309_215623_000000382045_00444_21039_0006.N1	DC map used
GOM_TRA_1PNPDE20060311_195657_000000402045_00472_21067_0000.N1	DC map used
GOM_TRA_1PNPDE20060311_195854_000000412045_00472_21067_0001.N1	DC map used
GOM_TRA_1PNPDE20060311_201106_000000442045_00472_21067_0002.N1	DC map used
GOM_TRA_1PNPDE20060311_201642_000000392045_00472_21067_0003.N1	DC map used
GOM_TRA_1PNPDE20060311_202004_000000352045_00472_21067_0004.N1	DC map used
GOM_TRA_1PNPDE20060311_203848_000000362045_00472_21067_0005.N1	DC map used
GOM_TRA_1PNPDE20060311_204631_000000362045_00472_21067_0006.N1	DC map used
GOM_TRA_1PNPDE20060312_210536_000000422045_00487_21082_0000.N1	DC map used
GOM_TRA_1PNPDE20060312_212800_000000382045_00487_21082_0001.N1	DC map used
GOM_TRA_1PNPDE20060312_213600_000000402045_00487_21082_0002.N1	DC map used
GOM_TRA_1PNPDE20060312_213907_000000392045_00487_21082_0003.N1	DC map used
GOM_TRA_1PNPDE20060312_214035_000000392045_00487_21082_0004.N1	DC map used
GOM_TRA_1PNPDE20060312_214747_000000362045_00487_21082_0005.N1	DC map used
GOM_TRA_1PNPDE20060312_215531_000000332045_00487_21082_0006.N1	DC map used
GOM_TRA_1PNPDE20060312_220037_000000342045_00487_21082_0007.N1	DC map used
GOM_TRA_1PNPDE20060312_220211_000000352045_00487_21082_0008.N1	DC map used
GOM_TRA_1PNPDE20060313_205404_000000372045_00501_21096_0000.N1	DC map used

GOM_TRA_1PNPDE20060313_205622_000000372045_00501_21096_0001.N1	DC map used
GOM_TRA_1PNPDE20060313_210418_000000412045_00501_21096_0002.N1	DC map used
GOM_TRA_1PNPDE20060313_210726_000000382045_00501_21096_0003.N1	DC map used
GOM_TRA_1PNPDE20060313_210855_000000392045_00501_21096_0004.N1	DC map used
GOM_TRA_1PNPDE20060313_211610_000000362045_00501_21096_0005.N1	DC map used
GOM_TRA_1PNPDE20060313_212355_000000342045_00501_21096_0006.N1	DC map used
GOM_TRA_1PNPDE20060313_221201_000000462046_00001_21097_0000.N1	DC map with no T dep.
GOM_TRA_1PNPDE20060313_221442_000000412046_00001_21097_0001.N1	DC map used
GOM_TRA_1PNPDE20060313_223439_000000372046_00001_21097_0002.N1	DC map used
GOM_TRA_1PNPDE20060313_223657_000000382046_00001_21097_0003.N1	DC map used
GOM_TRA_1PNPDE20060313_224453_000000392046_00001_21097_0004.N1	DC map used
GOM_TRA_1PNPDE20060313_224802_000000382046_00001_21097_0005.N1	DC map used
GOM_TRA_1PNPDE20060314_022542_000000352046_00003_21099_0000.N1	DC map used
GOM_TRA_1PNPDE20060314_023049_000000362046_00003_21099_0001.N1	DC map used
GOM_TRA_1PNPDE20060314_023223_000000352046_00003_21099_0002.N1	DC map used
GOM_TRA_1PNPDE20060314_023404_000000352046_00003_21099_0003.N1	DC map used
GOM_TRA_1PNPDE20060314_024216_000000552046_00003_21099_0004.N1	DC map used
GOM_TRA_1PNPDE20060314_025415_000000442046_00003_21099_0005.N1	DC map used
GOM_TRA_1PNPDE20060314_025740_000000532046_00003_21099_0006.N1	DC map used
GOM_TRA_1PNPDE20060314_200235_000000402046_00014_21110_0000.N1	DC map used
GOM_TRA_1PNPDE20060314_202227_000000372046_00014_21110_0001.N1	DC map used
GOM_TRA_1PNPDE20060314_202443_000000382046_00014_21110_0002.N1	DC map used
GOM_TRA_1PNPDE20060314_203236_000000392046_00014_21110_0003.N1	DC map used
GOM_TRA_1PNPDE20060314_203545_000000392046_00014_21110_0004.N1	DC map used
GOM_TRA_1PNPDE20060314_203714_000000392046_00014_21110_0005.N1	DC map used
GOM_TRA_1PNPDE20060314_204433_000000352046_00014_21110_0006.N1	DC map used
GOM_TRA_1PNPDE20060314_205218_000000342046_00014_21110_0007.N1	DC map used
GOM_TRA_1PNPDE20060320_201441_000000462046_00100_21196_0000.N1	DC map used
GOM_TRA_1PNPDE20060320_202305_000000482046_00100_21196_0001.N1	DC map used
GOM_TRA_1PNPDE20060320_203611_000000362046_00100_21196_0002.N1	DC map used
GOM_TRA_1PNPDE20060320_204338_000000372046_00100_21196_0003.N1	DC map used
GOM_TRA_1PNPDE20060320_204653_000000362046_00100_21196_0004.N1	DC map used
GOM_TRA_1PNPDE20060320_204823_000000392046_00100_21196_0005.N1	DC map used
GOM_TRA_1PNPDE20060320_205519_000000402046_00100_21196_0006.N1	DC map used
GOM_TRA_1PNPDE20060320_210350_000000362046_00100_21196_0007.N1	DC map used
GOM_TRA_1PNPDE20060321_194121_000000522046_00114_21210_0000.N1	DC map with no T dep.
GOM_TRA_1PNPDE20060321_194310_000000412046_00114_21210_0001.N1	DC map used
GOM_TRA_1PNPDE20060321_194531_000000302046_00114_21210_0002.N1	DC map used
GOM_TRA_1PNPDE20060321_195131_000000502046_00114_21210_0003.N1	DC map used
GOM_TRA_1PNPDE20060321_195306_000000462046_00114_21210_0004.N1	DC map used
GOM_TRA_1PNPDE20060321_200434_000000372046_00114_21210_0005.N1	DC map used
GOM_TRA_1PNPDE20060321_201157_000000382046_00114_21210_0006.N1	DC map used
GOM_TRA_1PNPDE20060321_201513_000000362046_00114_21210_0007.N1	DC map used
GOM_TRA_1PNPDE20060321_201644_000000382046_00114_21210_0008.N1	DC map used
GOM_TRA_1PNPDE20060323_201900_000000422046_00143_21239_0000.N1	DC map with no T dep.
GOM_TRA_1PNPDE20060323_202043_000000382046_00143_21239_0001.N1	DC map used
GOM_TRA_1PNPDE20060325_205638_000000462046_00172_21268_0000.N1	DC map with no T dep.
GOM_TRA_1PNPDE20060325_205815_000000422046_00172_21268_0001.N1	DC map used
GOM_TRA_1PNPDE20060325_210042_000000482046_00172_21268_0002.N1	DC map used
GOM_TRA_1PNPDE20060325_210553_000000502046_00172_21268_0003.N1	DC map used
GOM_TRA_1PNPDE20060325_210757_000000442046_00172_21268_0004.N1	DC map used
GOM_TRA_1PNPDE20060325_211806_000000412046_00172_21268_0005.N1	DC map used

GOM_TRA_1PNPDE20060325_211933_000000372046_00172_21268_0006.N1	DC map used
GOM_TRA_1PNPDE20060325_212628_000000382046_00172_21268_0007.N1	DC map used
GOM_TRA_1PNPDE20060325_212946_000000352046_00172_21268_0008.N1	DC map used
GOM_TRA_1PNPDE20060325_213118_000000362046_00172_21268_0009.N1	DC map used
GOM_TRA_1PNPDE20060326_202509_000000452046_00186_21282_0000.N1	DC map used
GOM_TRA_1PNPDE20060326_202643_000000432046_00186_21282_0001.N1	DC map used
GOM_TRA_1PNPDE20060326_202911_000000472046_00186_21282_0002.N1	DC map used
GOM_TRA_1PNPDE20060326_203451_000000462046_00186_21282_0003.N1	DC map used
GOM_TRA_1PNPDE20060326_203622_000000422046_00186_21282_0004.N1	DC map used
GOM_TRA_1PNPDE20060327_021706_000000362046_00189_21285_0000.N1	DC map used
GOM_TRA_1PNPDE20060327_022216_000000412046_00189_21285_0001.N1	DC map used
GOM_TRA_1PNPDE20060327_022353_000000412046_00189_21285_0002.N1	DC map used
GOM_TRA_1PNPDE20060327_022548_000000382046_00189_21285_0003.N1	DC map used
GOM_TRA_1PNPDE20060328_210246_000000442046_00215_21311_0000.N1	DC map with no T dep.
GOM_TRA_1PNPDE20060328_210415_000000402046_00215_21311_0001.N1	DC map used
GOM_TRA_1PNPDE20060328_210645_000000452046_00215_21311_0002.N1	DC map used
GOM_TRA_1PNPDE20060328_211146_000000462046_00215_21311_0003.N1	DC map used
GOM_TRA_1PNPDE20060328_211347_000000442046_00215_21311_0004.N1	DC map used
GOM_TRA_1PNPDE20060328_212343_000000392046_00215_21311_0005.N1	DC map used

The average DC inserted by the processor into the level 1b data products for the spectrometers SPA1 and SPB2 (per band: upper, central and lower) is plotted in fig. 4.5-1 and 4.5-2. From the figures, it can be noted that the DC is increasing at the expected rate: 400 electrons per year for SPA1 and 500 electrons per year for SPB2.

The same DC values are plotted in fig. 4.5-3 but for some occultations belonging only to the reporting month.

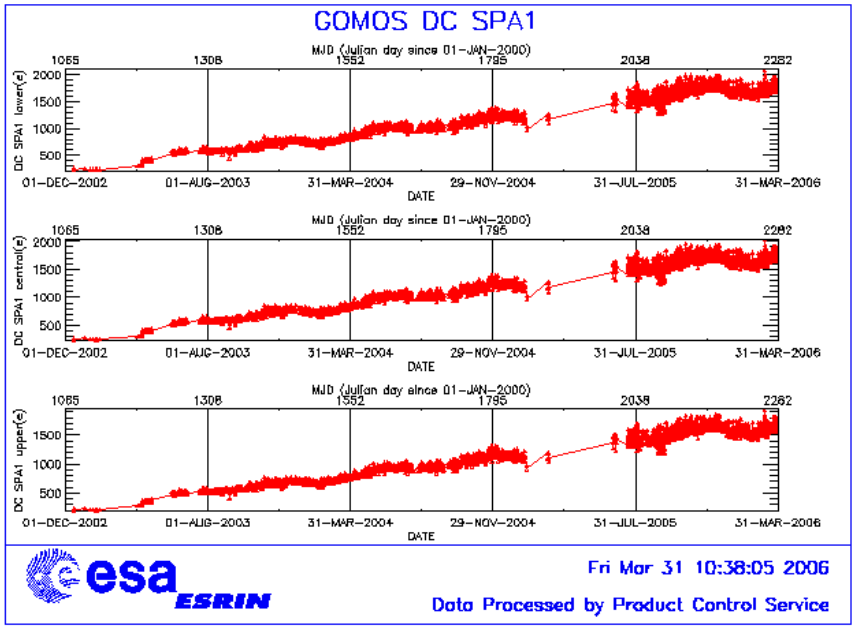

Figure 4.5-1: Mean DC evolution on SPA1 since 15th December 2002 until the end of the reporting period

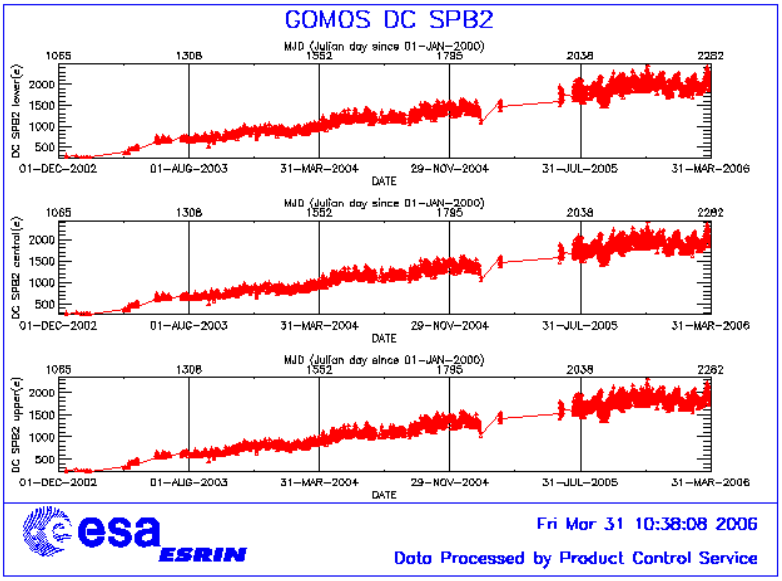

Figure 4.5-2: Mean DC evolution on SPB2 from 15th December 2002 until the end of the reporting period

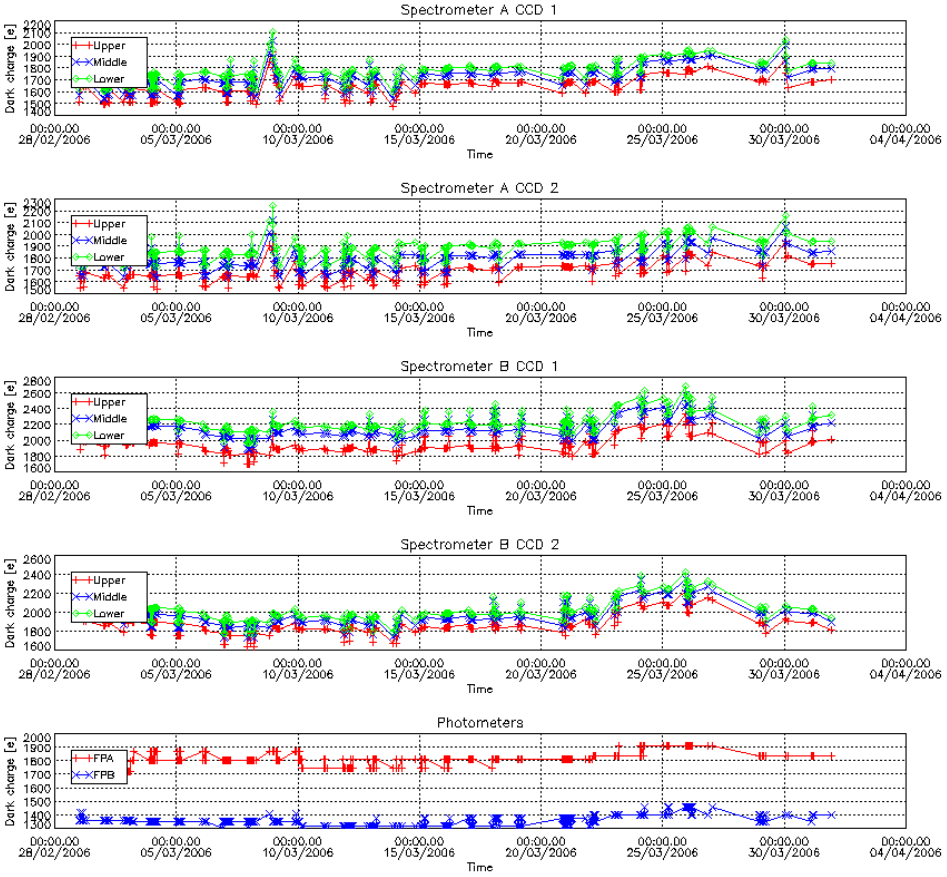

Figure 4.5-3: Mean Dark Charge of spectrometers and photometers during the reporting period

4.5.2 SIGNAL MODULATION

A parasitic signal was found to be systematically present, added to the useful signal, for the spectrometers A and B. The modulation is corrected in the data processing for spectrometers A1 and A2 (for spectrometer B it has much smaller amplitude and so is not corrected) and the modulation signal standard deviation is routinely monitored in order to detect any trend (fig. 4.5-4).

The modulation standard deviation, for every spectrometer, is characterised as follows:

$$\sigma_{mod} = (\text{'static noises'} - \text{'total static variance'})^{1/2} / \text{gain} \qquad \text{(in ADU)}$$

- The 'static noises' are calculated from the DSA observation performed once per orbit
- The 'total static variance' is obtained from ADF data (electronic chain noise, quantization noise).

The standard deviation of the modulation signal (fig. 4.5-4) shows high values during summer time for the ESRIN data, it now being confirmed that the South Atlantic Anomaly is the cause of these unexpected peaks. The quality of ESRIN data, in particular over the SAA zone, is impacted but the measure of this impact is under investigation. However, in the second half of October (both 2004 and 2005) the peaks are smaller because the DSA zone where the data are taken for this analysis is moving towards the Northern Hemisphere. At the end of October the DSA zone is definitely chosen by the planning system in the Northern Hemisphere (to fill the criteria 'DSA in full dark limb conditions') and the high peaks disappear.

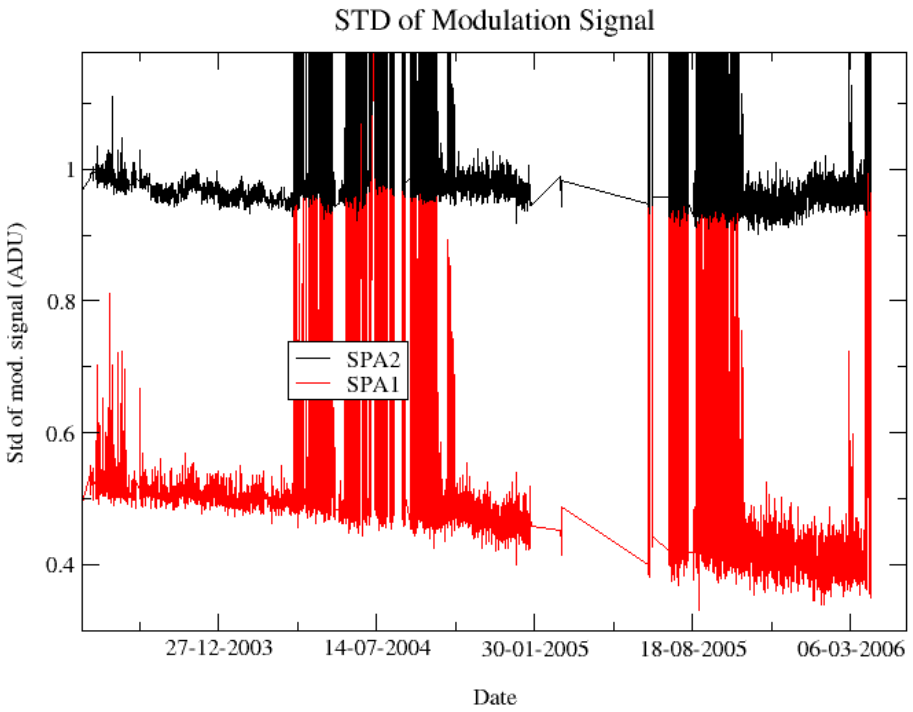

Figure 4.5-4: Standard deviation of the modulation signal

4.5.3 ELECTRONIC CHAIN GAIN AND OFFSET

No new electronic chain gain and offset calibration has been done during the reporting period so the results have been presented in previous MR.

The routine monitoring of the ADC offset is a good indicator of the ageing of the instrument electronics. During November 2005 an exercise has been done to analyze the variation of the ADC offset using the calibration observation in linearity mode performed on 28th November 2005.

The fig. 4.5-5 presents the evolution of the calibrated ADC offset for each spectrometer electronic chain. The unexpected increase of this offset seems to be due to an external contribution. In the ADC offset calibration procedure, linearity observations are used with two integration times of 0.25 and 0.50 seconds to extrapolate to an integration time of 0 seconds that gives the complete chain offset and not only the ADC offset. The complete offset contains any possible offsets, and especially the static dark charge (i.e. the dark charge that does not depend on the spectrometer integration time). If the memory area of the CCD is affected by the generation of hot pixels (this is confirmed by the presence of vertical lines visible in the measurement maps in spatial spread monitoring mode), it can be concluded that the increase observed in fig. 4.5-5 is due to these new hot pixels.

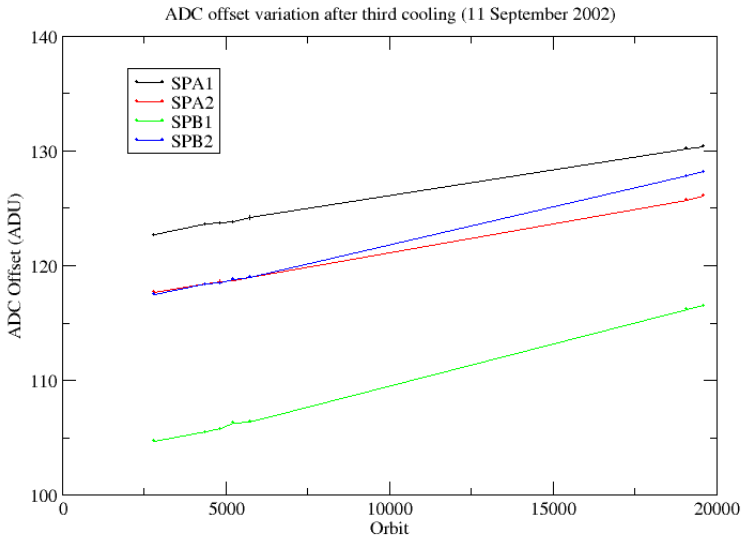

Figure 4.5-5: Evolution of the ADC offset for each spectrometer electronic chain

A current QWG task consists in completing the analysis to confirm that the offset increase is due to the dark charge increase in the memory area. This can be proven by the study of the noise due to the increased dark charge. The increase of ADC offset will be assumed to be equal to the increase of 'static dark charge' and the corresponding noise will be computed and compared to the increase of the residual of the signal variance.

If we keep the ADC offset constant, as it is also used to compute the dark charge at band level (which is used to correct the samples in the level 1b processing), the increase of the static dark charge - not taken into

account in the ADC offset - is compensated by an artificial increase of the calibrated dark charge. So, the star and limb spectra are correctly corrected for dark charge. A small bias can be added to the instrument noise due to the incorrect dark charge level. Anyway, this quantity is not large enough to require a modification of the ADC offset value.
An electronic chain gain calibration exercise has been performed. The values obtained have been compared with the ones written in the ADF and used by the operational IPF. The relative difference is much less than the 20% (threshold to change the ADF values) and thus no update of the gain is foreseen after this analysis.

4.6 Acquisition, Detection and Pointing Performance

4.6.1 SATU NOISE EQUIVALENT ANGLE

The Star Acquisition and Tracking Unit (SATU) noise equivalent angle (SATU NEA) consists of the statistical angular variation of the SATU data above the atmosphere. The mean of the standard deviation (STD over the 50 values per measurement) above 105 km are computed for every occultation, giving two values per occultation: one in the 'X' direction, one in the 'Y' direction. A mean value per day in every direction and limb is calculated and monitored in order to assess instrument performance in terms of star pointing (fig. 4.6-1). Also monthly averages are calculated and plotted (fig. 4.6-2). The thresholds are 2 and 3 micro radians in 'X' and 'Y' directions respectively.

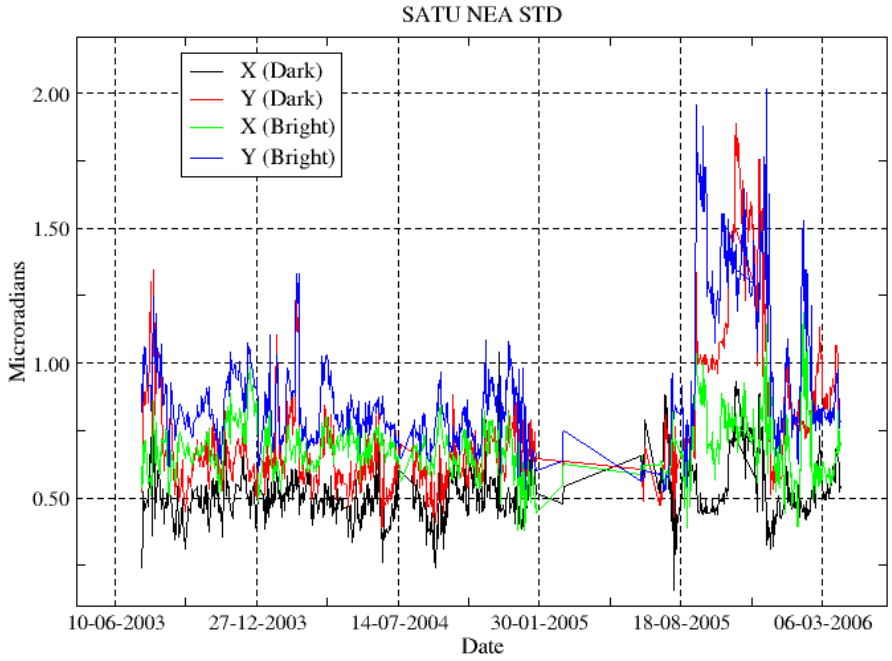

Figure 4.6-1: Average value per day of SATU NEA STD above 105 km

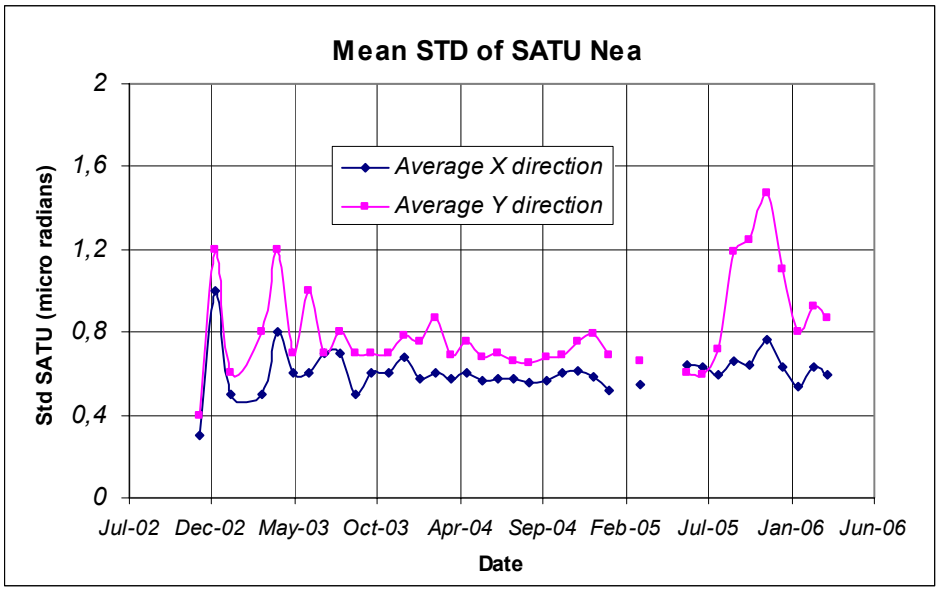

Figure 4.6-2: Average value per month of SATU NEA STD above 105 km

Before May 2003, data above 90 km have been considered (instead of 105 km) but from May 2003 on, data taken in the mesospheric oxygen layer (located around 100 km altitude) have been avoided because they could cause fluctuations on the SATU data. Also the products with errors (error flag set) are discarded from May 2003 onwards. As can be seen in fig. 4-6.1, the SATU NEA had a sudden increase on 8th September 2005 mainly in 'Y' axis. These values remained high, fluctuating between 1 and 1.8 microrad until December 2005 when they came back to the values they used to be before the increase of September. The cause of this unexpected behavior is under investigation although the values were always below the threshold and the data quality was not affected.

The results for some occultations belonging to previous months (monthly averages) are presented in fig. 4.6-2, where the change in trend in September 2005, mainly for the 'Y' axis is visible.

4.6.2 TRACKING LOSS INFORMATION

This verification consists of the monitoring of the tangent altitude at which the star is lost. It is an indicator of the pointing performance although it is to be considered that star tracking is also lost due to the presence of clouds and hence not only due to deficiencies in the pointing performance. Therefore, only the detection of any systematic long-term trend is the main purpose of this monitoring. The recent results are presented in fig. 4.6-3 and 4.6-4:

- The dependence of the altitude at which tracking is lost on the magnitude of the star is very small because the tracking is mainly lost due to the refraction and the scintillation that depend on the atmospheric conditions.
- The azimuth of some stars could be very near to the reduced instrument azimuth edges and therefore there could be occultations planned to have a duration very small (2, 6, 10…seconds).To avoid planning this kind of useless occultation, it has been decided to set the minimum occultation duration

value to 25 seconds. Fig. 4.6-3 (dark limb) shows stars lost at 50-60 km which corresponds with durations around 25 seconds.

- In bright limb it is not expected that the occultations are lost at very low altitudes due to the amount of light arriving to the pointing system mainly when the refraction effects start to be important. We see from fig. 4.6-4 that there are few stars lost at altitudes around 4 km. This occurs when the pointing system is not able to point to the star anymore but, instead of finishing the occultation, it continues to track light until the planned duration is reached.
- Daily statistics are given in fig. 4.6-5 (calculated using 50 products per day). The high peaks in standard deviation before 25th January 2005, are due to the long lasting occultations or partial occultations (the entire occultation is included within the following orbit data). The ones during June/July/August 2005 are due to the tests performed for the anomaly investigation. After 29th August (GOMOS operational again) the peaks are due to the "short occultations".
- Monthly statistics are given in fig. 4.6-6 (calculated using 50 products per day) where the change in trends, mainly for dark limb, is visible for the period of GOMOS testing.

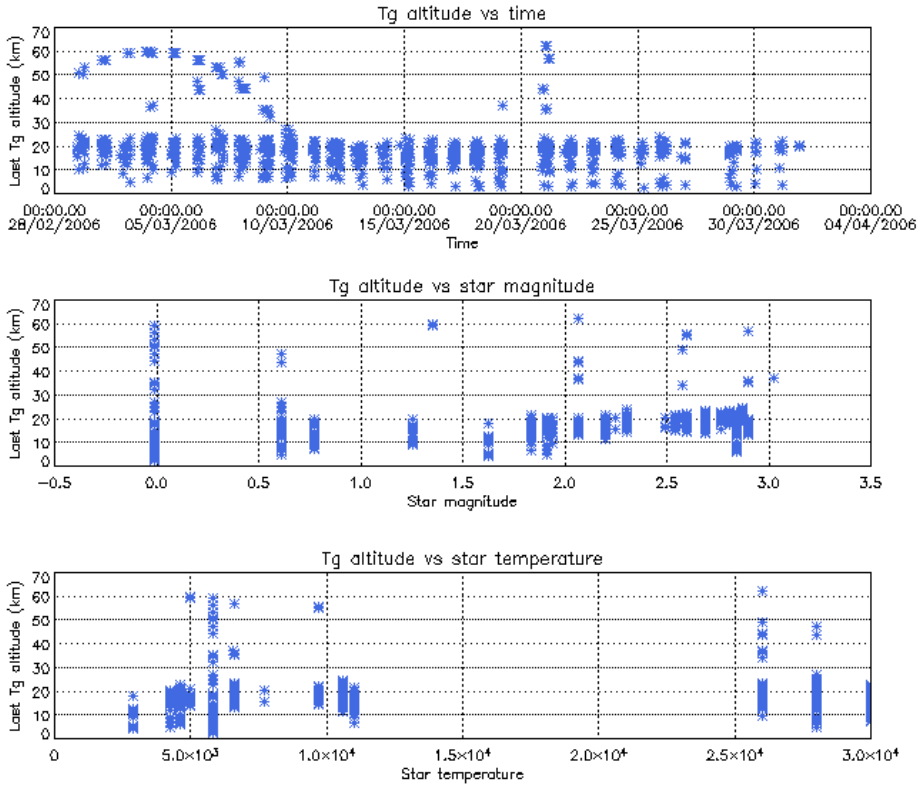

Figure 4.6-3: Last tangent altitude of the occultation (dark limb), point at which the star is lost

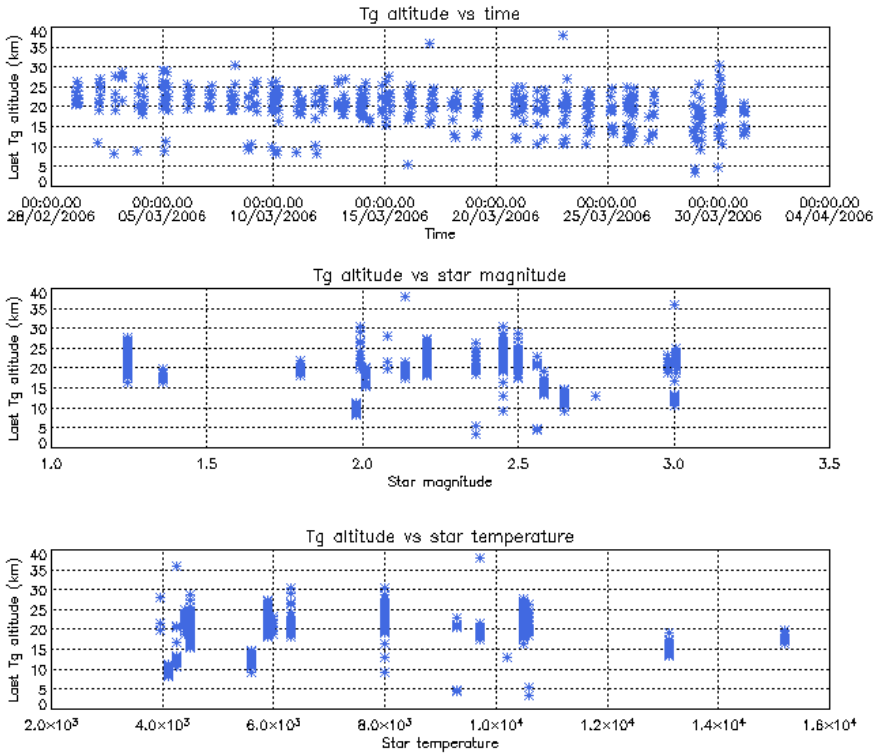

Figure 4.6-4: Last tangent altitude of the occultation (bright limb), point at which the star is lost

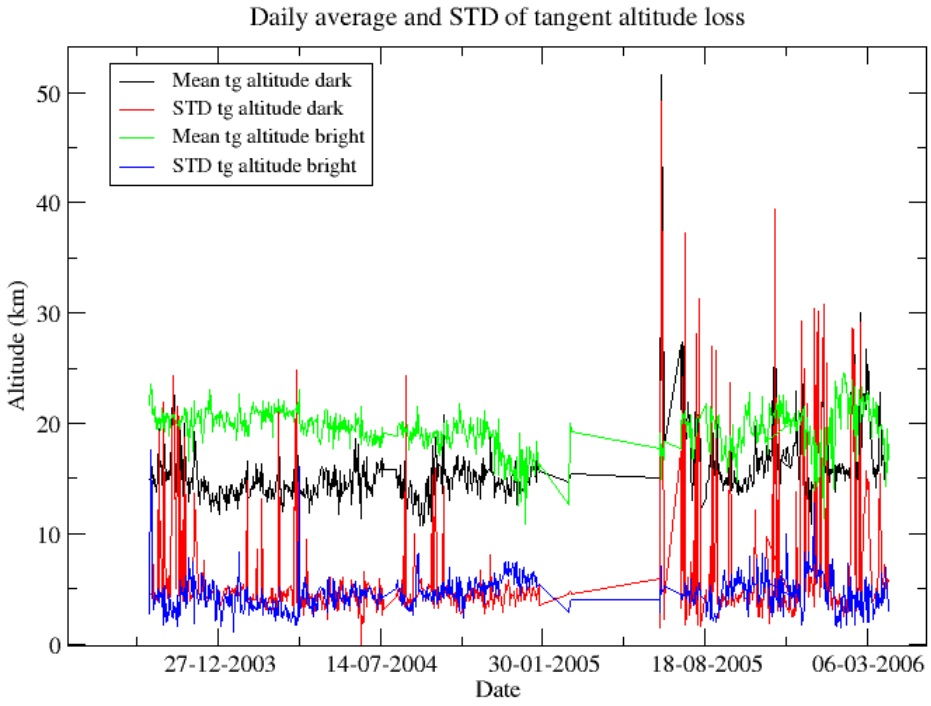

Figure 4.6-5: Daily average and STD of tangent altitude loss for the reporting period

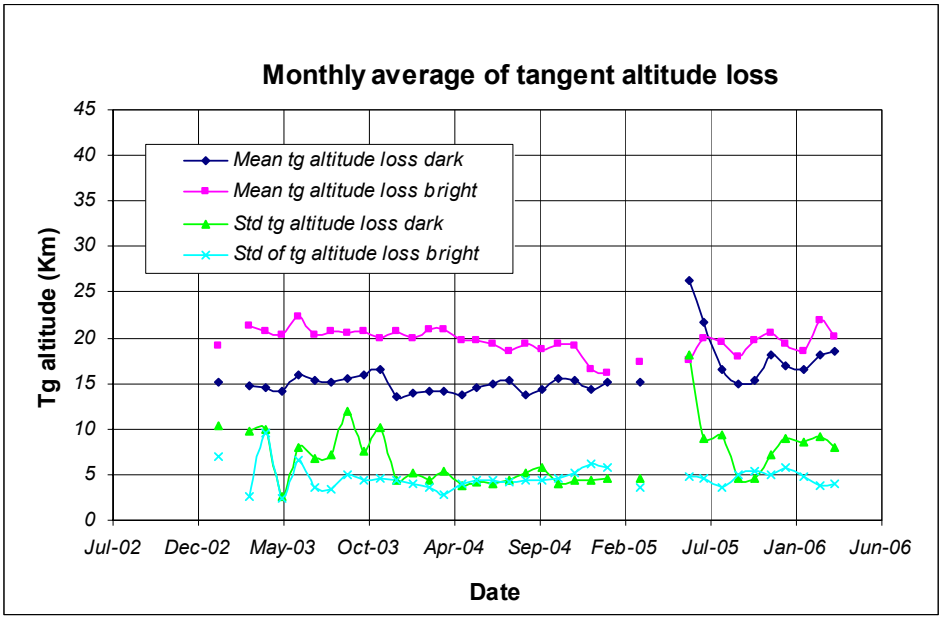

Figure 4.6-6: Monthly mean tangent altitude (and STD) at which the star is lost since January 2003

4.6.3 MOST ILLUMINATED PIXEL (MIP)

The MIP (Most Illuminated Pixel) is the star position on the SATU CCD in detection mode and it is recorded in the housekeeping data. The nominal centre of the SATU is pixel number **145** in elevation and number **205** in azimuth. The detection of the stars should not be far from this centre. As it can be seen in fig. 4.6-7 the **azimuth MIP** was within the threshold (table 4.6-1) since September 2002 until the occurrence of the anomaly on January 2005, even if a small variation is present. The reason for the change in trend observed after the anomaly is, at the moment, not understood. The **elevation MIP** had a significant variation (see the *note* below) until 12th December 2003 when a new PSO algorithm was activated in order to reduce the deviations of the ENVISAT platform attitude with respect to the nominal one. Similarly to the azimuth, after the anomaly of January 2005 the Elevation MIP has a drift that has no explanation. Investigations are ongoing to try to understand this behavior of the MIP as, although it does not impact the data quality or the star location on the CCD array during the measurements, it may invalidate attitude monitoring by GOMOS and could represent a hidden anomaly.

Note: A MIP variation onto the SATU CCD of 50 pixels corresponds to a de-pointing of 0.1 degrees

Table 4.6-1: MIP Thresholds

MIP X	**Mean delta Az**	[198 - 210]
	Std delta Az	7
MIP Y	**Mean delta El**	[140 – 150]
	Std delta El	4

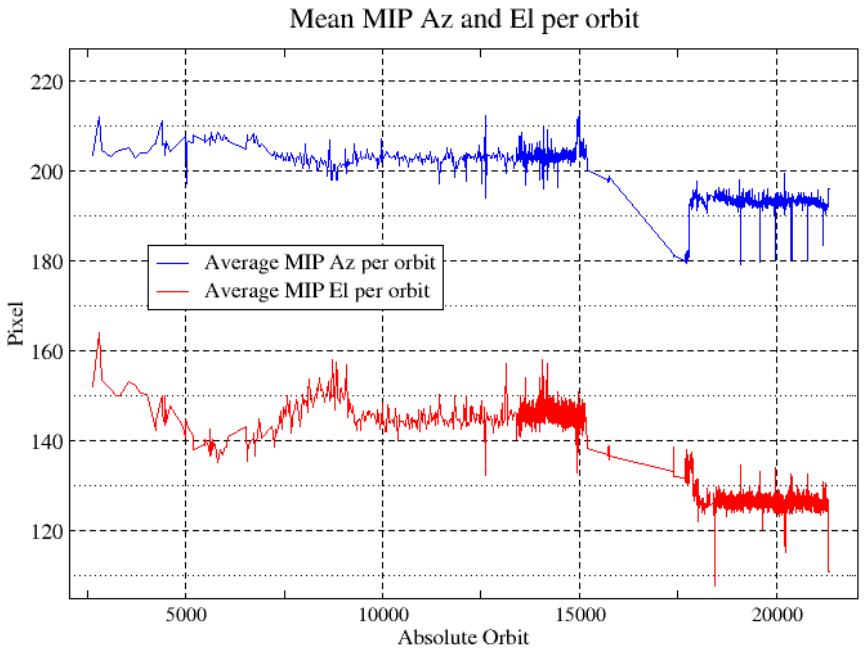

Figure 4.6-7: Mean values of MIP for some orbits since 1st September 2002 (see table 4.6-1)

Fig. 4.6-8 shows the standard deviation of azimuth and elevation MIP that should be within the thresholds of table 4.6-1. The peaks observed mean that one (or more) stars were detected very far from the SATU detection point and, in this case, the stars were lost during the centering phase (see section 3.2 for stars lost in centering).

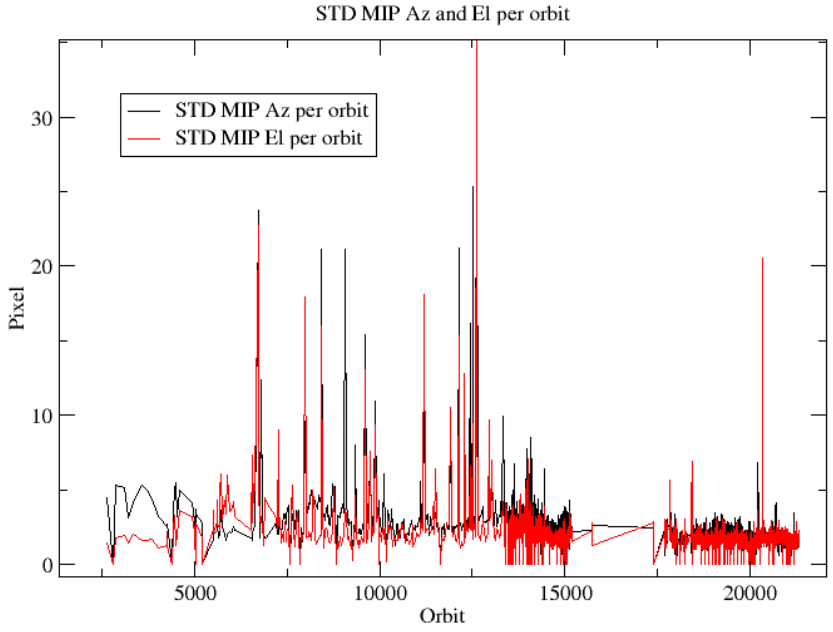

Figure 4.6-8: Standard deviation of MIP Azimuth and Elevation for some orbits since 1st September 2002 until end of reporting period (see table 4.6-1)

5 LEVEL 1 PRODUCT QUALITY MONITORING

5.1 Processor Configuration

5.1.1 VERSION

About 23% of near real time GOM_TRA_1P products have been received by the DPQC team for routine quality control and long term trend quality monitoring. The current level 1-processor software version for the operational ground segment is GOMOS/4.02 (see table 5.1-1). The product specification is PO-RS-MDA-GS2009_10_3H. This processor has been cleared for initial level 1 data release, with a disclaimer for known artefacts (http://envisat.esa.int/dataproducts/availability/disclaimers) that are currently being resolved and will be implemented in the next release (http://envisat.esa.int/dataproducts/availability).

Users are supplied with 2002-2005 data sets reprocessed by the last prototype processor GOPR_6.0c_6.0f developed and operated by ACRI. See table 5.1-2 for prototype level 1b versions and modifications. The next GOMOS operational ground segment version (GOMOS/5.00) will be in line with the prototype version used for this second reprocessing.

Table 5.1-1: PDS level 1b product version and main modifications implemented

Date	Version	Description of changes
23-MAR-2004	Level 1b version 4.02 at PDHS-E and PDHS-K	Algorithm baseline level 1b DPM 6.0 • Adding a new calibration parameters (these values are hard coded at the moment) • Removal of redundancy chain from code • Modifications in the processing to apply new configuration and calibration parameter • New algorithm to determine between dark, twilight and bright limb and to handle data accordingly • Added handling of source packages with invalid packet header • Added enumerations for all configuration flags
31-MAY-2003	Level 1b version 4.00 at PDHS-E and PDHS-K	Algorithm baseline level 1b DPM 5.4: • Modulation correction step added after the cosmic rays detection processing • Inversion of the non-linearity and offset corrections • Modification of the computation of the estimated background signal measured by the photometers: use the spectrometer radiometric sensitivity curve and the photometer transfer function. • Use of the dark charge map at orbit level computed from the DSA (dark sky area) if any in the level 0 product • Implementation of a new unfolding algorithm for the photometer samples
21-NOV-2002	Level 1b version 3.61 at PDHS-E and PDHS-K	Algorithm baseline DPM 5.3: • Review of some default values • New definition of one PCD flag (atmosphere) • Temporal interpolation of ECMWF data

Table 5.1-2: GOPR level 1b product version and main modifications implemented

Date	Version	Description of changes
22-JUL-2005	GOPR_6.0c	Level 1b: • Correction of FP unfolding algorithm • Background correction of SPB in full dark limb • Modification of the computation of the incidence angle • Correction of the flat-field correction equations • Star spectrum location on CCD modified for SPB Configuration for second reprocessing: • Use of new reflectivity LUT • New wavelength assignment for SPA1, A2, B1 • Spatial PSF of SPB modified
17-MAR-2004	GOPR 6.0a	• Provide SFA and SATU angles in degrees • Elevation angle dependency of the reflectivity LUT added in the algorithms • Ratio upper/star signal added (FLAGUC) • Add Dark Charge used for dark charge correction (per band) • Flag for illumination condition (PCDillum) • Minimum sample value for which the cosmic rays detection processing is applied (Crmin) is a function of gain index • Logic for computation of the flags attached to the reference star spectrum (Flref) modified • Add the computation of the sun direction in the inertial geocentric frame to be written in the level 1b and limb products. • Spectrometer effective sampling time added
25-JUL-2003	GOPR 5.4f	• The demodulation process is applied only in full dark limb and twilight limb conditions.
17-JUL-2003	GOPR 5.4e	• Sun zenith angle is computed in the geolocation process. The occultation is now classified into (0) full dark limb condition, (1) bright limb condition and (2) twilight limb condition. • No background correction applied in full dark limb condition. The location of the image of the star spectrum on the CCD array is no more aligned with the CCD lines.
02-JUL2003	GOPR 5.4d	• The maximum number of measurements is set to 509 (instead of 510) in the GOPR prototype.
17-MAR-2003	GOPR 5.4c	• Modification of the CAL ADFs (update of the limb radiometric LUT). The products are affected only if the limb spectra are converted into physical units • Modifications to allow compatibility with ACRI computational cluster (no modifications of the results) • Modification of the logic to handle dark charge map refresh at orbit level (DSA data is now directly processed by the level 1b processor if available in the level 0 product). No impact on the results
21-FEB-2003	GOPR 5.4b	• DC map values are rounded when written in the level 1b product • Modification of the CAL ADFs (update of the wavelength assignment of SPB1 and SPB2) • Modify the computation of flag_mod in the modulation correction routine
17-JAN-2003	GOPR 5.4a	• use the start and stop dates of the occultation when calling the CFI □nterpol instead of start and stop dates of the level 0 product • modify the ECMWF filename information in the SPH of the level 1b and limb products

5.1.2 AUXILIARY DATA FILES (ADF)

The ADF's files in tables 5.1-3, 5.1-4, 5.1-5, 5.1-6 and 5.1-7 have been disseminated to the PDS during the whole mission. Note that the files outlined in yellow are the set of auxiliary files used during the reporting period. For every type of file, the validity runs from the start validity time until the start validity time of the following one, but if an ADF file has been disseminated after the start validity time, it is obvious that it will be used by the PDHS-E and PDHS-K PDS only after the dissemination time (this happens the majority of the time). Just like the other ADF's, the calibration auxiliary file (GOM_CAL_AX) has been updated several times in the past (table 5.1-7) but the difference is that now it is updated in a weekly basis with only new DC maps, and that is why the files used during March 2006 are reported in a separate table (table 5.1-8) that changes from report to report.

Table 5.1-3: Table of historic GOM_PR1_AX files used by PDS for level 1b products generation. The GOM_PR1_AX is a file containing the configuration parameters used for processing from level 0 to level 1b products

Used by PDS for Level 1b products generation in period	GOM_PR1_AX (GOMOS processing level 1b configuration file)
01-MAR-2002 → 29-MAR-2002	**GOM_PR1_AXVIEC20020121_165314_20020101_000000_20200101_000000** • Pre-launch configuration
30-MAR-2002 → 14-NOV-2002	**GOM_PR1_AXVIEC20020329_115921_20020324_200000_20100101_000000** • Changed num_grid_upper, thr_conv and max_iter in the atmospheric GADS
Not used	**GOM_PR1_AXVIEC20020729_083756_20020301_000000_20100101_000000** • Cosmic Ray mode + threshold • DC correction based on maps • Non-linearity correction disabled
Not used	**GOM_PR1_AXVIEC20021112_170331_20020301_000000_20100101_000000** • Central background estimation by linear interpolation + associated thresholds
15-NOV-2002 → 26-MAR-2003	**GOM_PR1_AXVIEC20021114_153119_20020324_000000_20100101_000000** • Same content as GOM_PR1_AXVIEC20021112_170331_20020301_000000_20100101_000000 but validity start updated so as to supersede according to the PDS file selection rules GOM_PR1_AXVIEC20020329_115921_20020324_200000_20100101_000000
27-MAR-2003 → 19-MAR-2004	**GOM_PR1_AXVIEC20030326_085805_20020324_200000_20100101_000000** • Same content as GOM_PR1_AXVIEC20021112_170331_20020301_000000_20100101_000000 but validity start updated so as to supersede according to the PDS file selection rules GOM_PR1_AXVIEC20020329_115921_20020324_200000_20100101_000000
20-MAR-2004 → 22-MAR-2004	**GOM_PR1_AXVIEC20040319_134932_20020324_200000_20100101_000000** • Ray tracing parameter changed: convergence criteria set to 0.1 microrad

23-MAR-2004 → 01-APR-2004 *Notes*: • This file was constructed from GOM_PR1_AXVIEC20030326_085805_20020324_200000_20100101_000000 (so without the ray tracing parameter changed) • This file was used by the GOMOS/4.02 processors before the IECF dissemination. The dissemination was done on 25th March 2004	**GOM_PR1_AXVIEC20040316_144850_20020324_200000_20100101_000000** GOM_PR1 ADF for version GOMOS/4.02, changes: • The central band estimation mode • Atmosphere thickness • Altitude discretisation
02-APR-2004	**GOM_PR1_AXVIEC20040401_083133_20020324_200000_20100101_000000** • Ray tracing parameter changed: convergence criteria set to 0.1 microrad

Table 5.1-4: Table of historic GOM_INS_AX files used by PDS for level 1b products generation. The GOM_INS_AX is a file containing the characteristics of the instrument and it is used for processing from level 0 to level 1b products and from level 1b to level 2 products

Used by PDS for Level 1b products generation in period	GOM_INS_AX (GOMOS instrument characteristics file)
01-MAR-2002 → 29-JUL-2002	**GOM_INS_AXVIEC20020121_165107_20020101_000000_20200101_000000** • Pre-launch configuration
30-JUL-2002 → 12-NOV-2002	**GOM_INS_AXVIEC20020729_083625_20020301_000000_20100101_000000** • Factors for the conversion of the SFA angles from SFM axes to GOMOS axes
13-NOV-2002 → 16-JUL-2003	**GOM_INS_AXVIEC20021112_170146_20020301_000000_20100101_000000** • No more invalid spectral range
Not used	**GOM_INS_AXVIEC20030716_080112_20030711_120000_20100101_000000** • New value for SFM elevation zero offset for redundant chain: 10004
17-JUL-2003	**GOM_INS_AXVIEC20030716_105425_20030716_120000_20100101_000000** • Bias induct azimuth redundant value set to -0.0084 rad (-0.4813 deg)

Table 5.1-5: Table of historic GOM_CAT_AX files used by PDS for level 1b products generation. The GOM_CAT_AX is a file holding the star catalogue used for processing from level 0 to level 1b products

Used by PDS for Level 1b products generation in period	GOM_CAT_AX (GOMOS Stat Catalogue file)
01-MAR-2002	**GOM_CAT_AXVIEC20020121_161009_20020101_000000_20200101_000000** • Pre-launch configuration

Table 5.1-6: Table of historic GOM_STS_AX files used by PDS for level 1b products generation. The GOM_STS_AX is a file containing star spectra used for processing from level 0 to level 1b products

Used by PDS for Level 1b products generation in period	GOM_STS_AX (GOMOS Star Spectra file)
01-MAR-2002	**GOM_STS_AXVIEC20020121_165822_20020101_000000_20200101_000000** • Pre-launch configuration

Table 5.1-7: Table of historic GOM_CAL_AX files used by PDS for level 1b products generation. The GOM_CAL_AX is a file containing the calibration parameters used for processing from level 0 to level 1b products

Used by PDS for Level 1b products generation in period	GOM_CAL_AX (GOMOS Calibration file)
01-MAR-2002 → 29-JUL-2002	**GOM_CAL_AXVIEC20020121_164808_20020101_000000_20200101_000000** • Pre-launch configuration
Not used	**GOM_CAL_AXVIEC20020121_142519_20020101_000000_20200101_000000** • Pre-launch configuration
30-JUL-2002 → 12-NOV-2002	**GOM_CAL_AXVIEC20020729_082426_20020717_193500_20100101_000000** • Band setting information • Wavelength assignment • Spectral dispersion LUT • ADC offset for Spectrometers • PRNU maps • Thermistor coding LUT • DC maps
Not used	**GOM_CAL_AXVIEC20021112_165603_20020914_000000_20100101_000000** • Band setting information • DC maps • PRNU maps • Wavelength assignment • Spectral dispersion LUT • Radiometric sensitivity LUT (star and limb) • SP-FP intercalibration LUT • Vignetting LUT • Reflectivity LUT • ADC offset
13-NOV-2002 → 30-JAN-2003	**GOM_CAL_AXVIEC20021112_165948_20021019_000000_20100101_000000** • Only DC maps updated
31-JAN-2003 → 11-APR-2003	**GOM_CAL_AXVIEC20030130_133032_20030101_000000_20100101_000000** • Only DC maps updated (using DSA of orbit 04541)
12-APR-2003 → 02-JUN-2003	**GOM_CAL_AXVIEC20030411_065739_20030407_000000_20100101_000000** • Modification of the radiometric sensitivity curve for the limb spectra. Note that the modification of this LUT has no impact on the GOMOS processing. The LUT is just copied into the level 1b limb product for user conversion purpose. • Updated DC map only (using DSA of orbit 05762).
03-JUN-2003: from this date onwards, mainly updates to DC maps are done. Every month, the table of new GOM_CAL files with **only** DC maps updated is provided (table 5.1-8). Eventual changes to this file not corresponding only to DC maps updates will be reported in this table.	**GOM_CAL_AXVIEC20030602_094748_20030531_000000_20100101_000000** • Updated DC maps only (using DSA of orbit 06530)
13-FEB-2004 → 23-FEB-2004	**GOM_CAL_AXVIEC20040212_103916_20040209_000000_20100101_000000** • Update of the reflectivity LUT • Updated DC maps (Orbit 10194, date 11-FEB-2004)

Table 5.1-8: Calibration ADF for reporting period. These files are updated (only with DC maps) in a 8-10 days basis

Used by PDS for Level 1b products generation in period	GOM_CAL_AX (GOMOS Calibration file)
22-FEB-2006 → 02-MAR-2006	**GOM_CAL_AXVIEC20060221_093830_20060218_000000_20100101_000000** (orbit 20788, date 20 FEB 2006)
03-MAR-2006 → 09-MAR-2006	**GOM_CAL_AXVIEC20060302_100214_20060228_000000_20100101_000000** (orbit 20922, date 01 MAR 2006)
10-MAR-2006 → 21-MAR-2006	**GOM_CAL_AXVIEC20060309_155255_20060307_000000_20100101_000000** (orbit 21023, date 08 MAR 2006)
22-MAR-2006 → 31-MAR-2006	**GOM_CAL_AXVIEC20060321_083359_20060319_000000_20100101_000000** (orbit 21195, date 20 MAR 2006)

5.2 Quality Flags Monitoring

In this section, the results of monitoring some Product Quality information stored in level 1b products that did not have a fatal error (MPH error flag not set) are discussed. The products with fatal errors were around 0.4% of the products received during the reporting month for the quality monitoring.

On the one hand, for every product we have information of the **number of measurements** where a given problem was detected (i.e. number of invalid measurements, number of measurements containing saturated samples, number of measurements with demodulation flag set…). On the other hand, there are **flags** that indicate problems within the product (i.e. flag set to one if the reference spectrum was computed from DB, flag set to zero if SATU data were not used…).

For the information on the number of measurements a plot of percentages with respect to time is provided in fig. 5.2-1. Part of this information, the most relevant one, is also plotted in a world map as a function of ENVISAT position: % of cosmic ray hits per profile, % of datation errors per profile, % of star falling outside the central band per profile and % of saturation errors per profile (fig.5-2.2).

It can be seen from fig. 5.2-1 that the cosmic rays hits occurred several times for the 95% of the measurements of the products. Looking at fig. 5.2-2 it can be clearly observed that this high percentage occurred when the satellite crossed the South Atlantic Anomaly (SAA) zone. The percentage of saturation errors per profile shows a slight increase over the SAA zone.

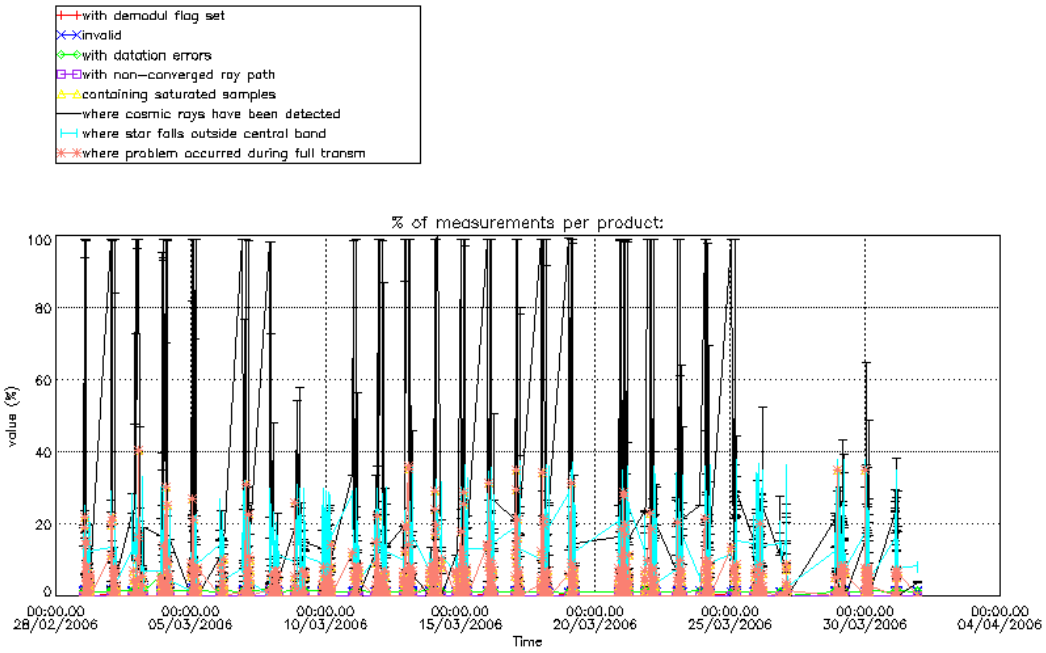

Figure 5.2-1: Level 1b product quality monitoring with respect to time

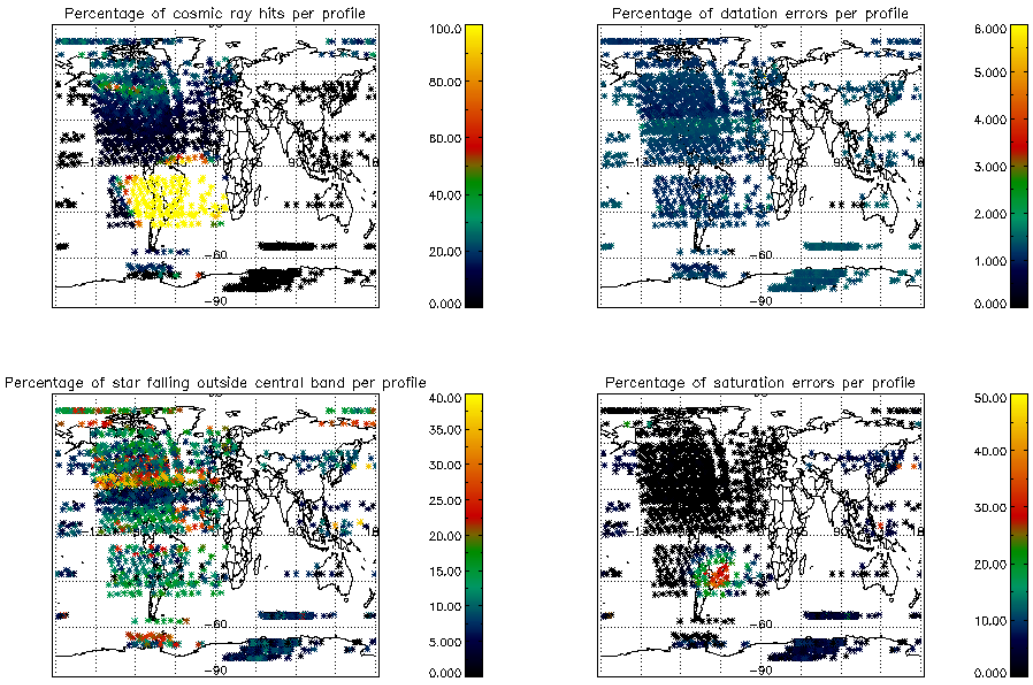

Figure 5.2-2: Level 1b product quality monitoring with respect to geolocation of ENVISAT

The other values (% of invalid measurements per product, % of measurements per product with datation errors…) are quite low.

The flag information is given in table 5.2-1. The percentage of the products that have at least one measurement with demodulation flag set is also reported.

Table 5.2-1: Percentage of products during the reporting period with:

At least one measurement with demodulation flag set:	12 %
Reference spectrum computed from DB:	0.0 %
Reference spectrum with small number of measurements:	0.0 %
SATU data not used:	0.0 %

5.2.1 QUALITY FLAGS MONITORING (EXTRACTED FROM LEVEL 2 PRODUCTS)

In this section, the Product Quality information coming from the level 1 processing but stored also in the level 2 products is plotted. Only products that did not have a fatal error (MPH error flag not set) are considered. The purpose of using the level 2 data is simply that the percentage of level 2 products arriving to the DPQC team for the quality monitoring is much higher. For the reporting month, 70% of the archived products have been received. The plots are very similar to fig. 5.2-1 and 5.2-2 (demodulation flag information is not included) but separating ascending from descending passes (see table 5.2-2). Fig. 5.2-3 and 5.2-4 present some quality information as a function of the time whereas in fig. 5.2-5 and 5.2-6 the plot is respect to the satellite position at the beginning of the occultations.

Table 5.2-2: Latitude of the different limb illumination in ascending and descending passes

Ascending	**Dark:** [-30^o, 60^o] **Twilight:** below -30^o , above 60 ^{o} **Bright:** above 70^o
Descending	**Dark:** No **Twilight:** No **Bright:** All

In ascending (fig. 5.2-3) the percentage of measurements “where a problem occurred during the full transmission” per product is around 2% while for the descending passes (fig. 5.2-4) is around 10%. This is due to the saturation that occurs mainly in bright limb. In ascending the saturation occurs over the SAA zone but it is quite low elsewhere. From fig. 5.2-3 (twilight/night-side of the orbit) you can see also that, for many products, 25-30 % of the measurements have the star signal falling outside the central band. In the descending part (day-side of the orbit) the percentage is around 10-15 % (fig. 5.2-4). This is because during the night the stars are lost deeper within the atmosphere and the turbulence phenomena become more important, producing the star to be less ‘focused’ on the spectrometers central band.

In ascending (fig. 5.2-5) the SAA is perfectly localized by the high percentage of cosmic ray hits per product (upper left panel). It is not the same if we look at fig. 5.2-6, because in descending most of the

occultations are in bright limb conditions (see table 5.2-2) and the cosmic rays detection processing is not activated.

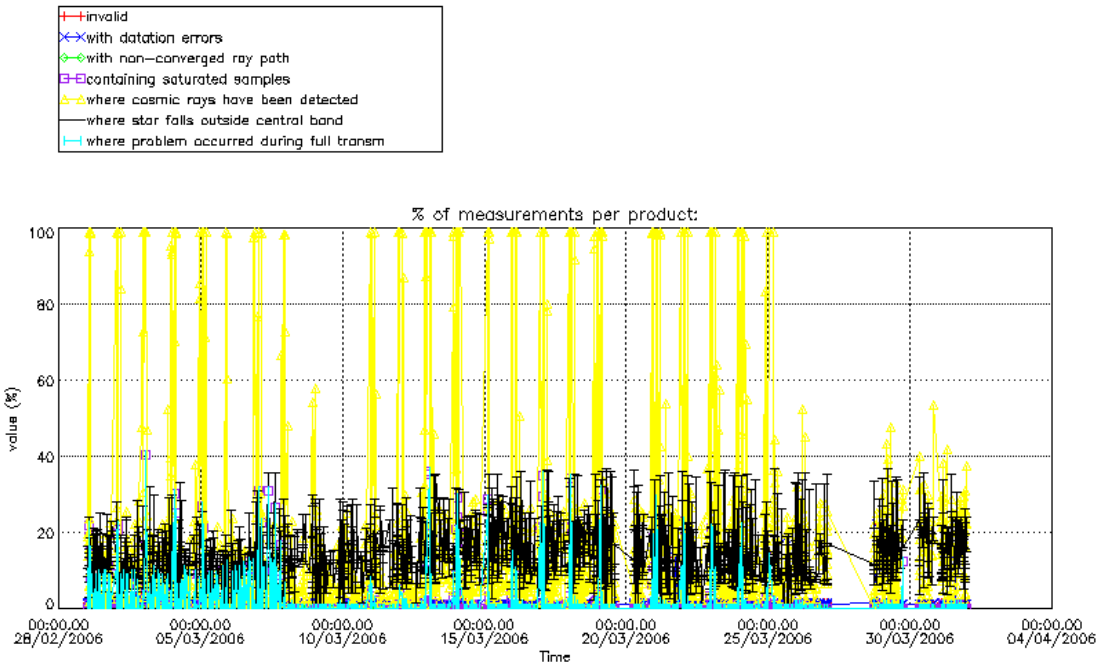

Figure 5.2-3: Level 1b product quality monitoring with respect to time <u>ASCENDING</u> ENVISAT passes

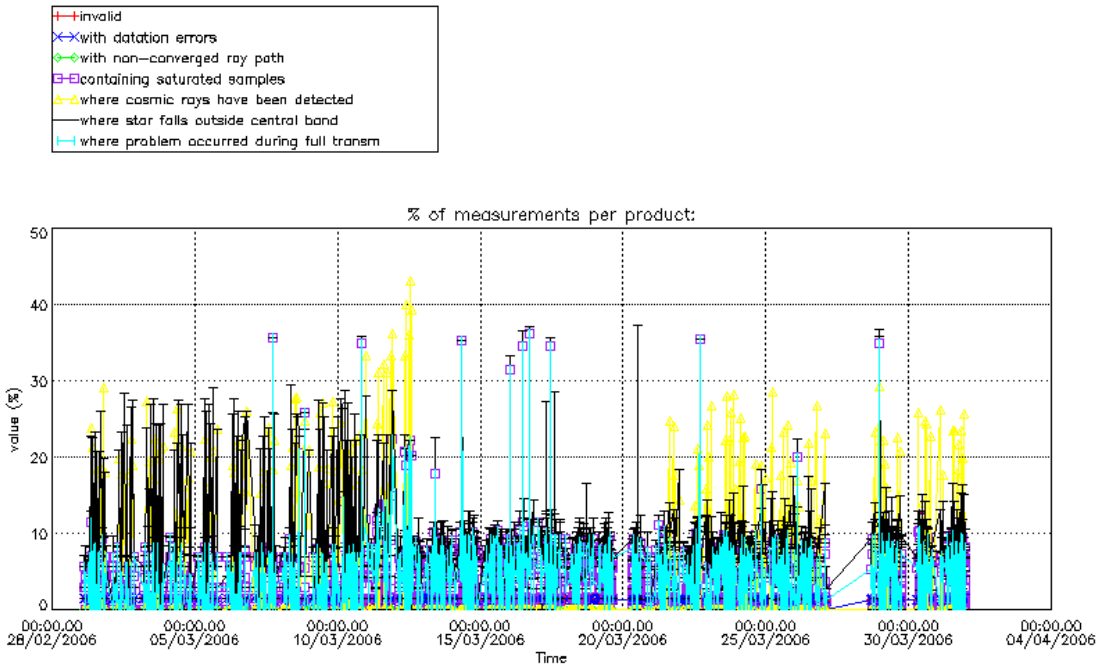

Figure 5.2-4: Level 1b product quality monitoring with respect to time <u>DESCENDING</u> ENVISAT passes

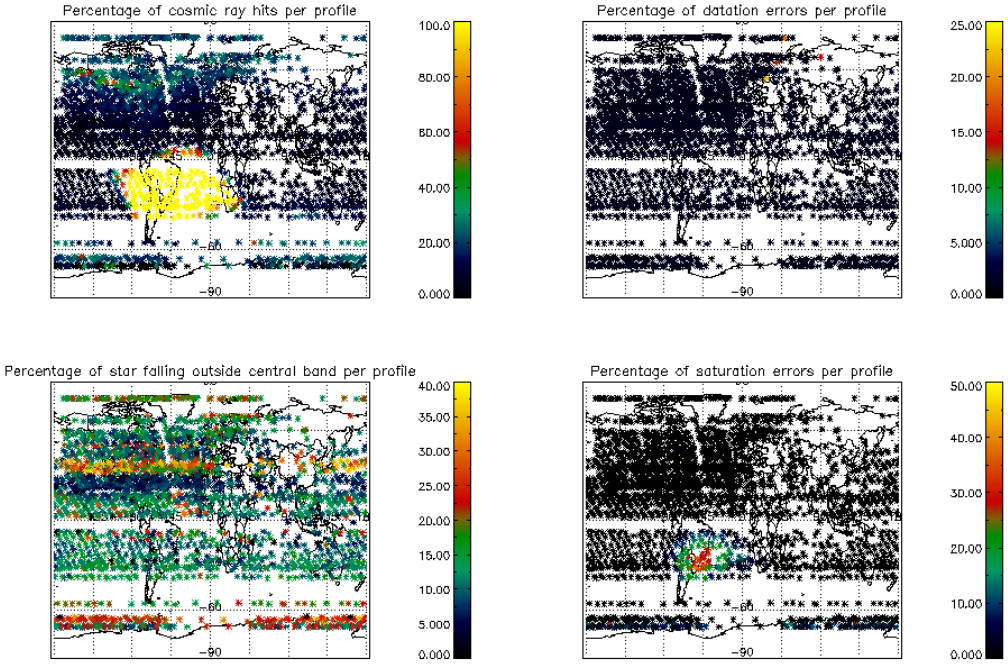

Figure 5.2-5: Level 1b product quality monitoring with respect to geo-location for ASCENDING ENVISAT passes

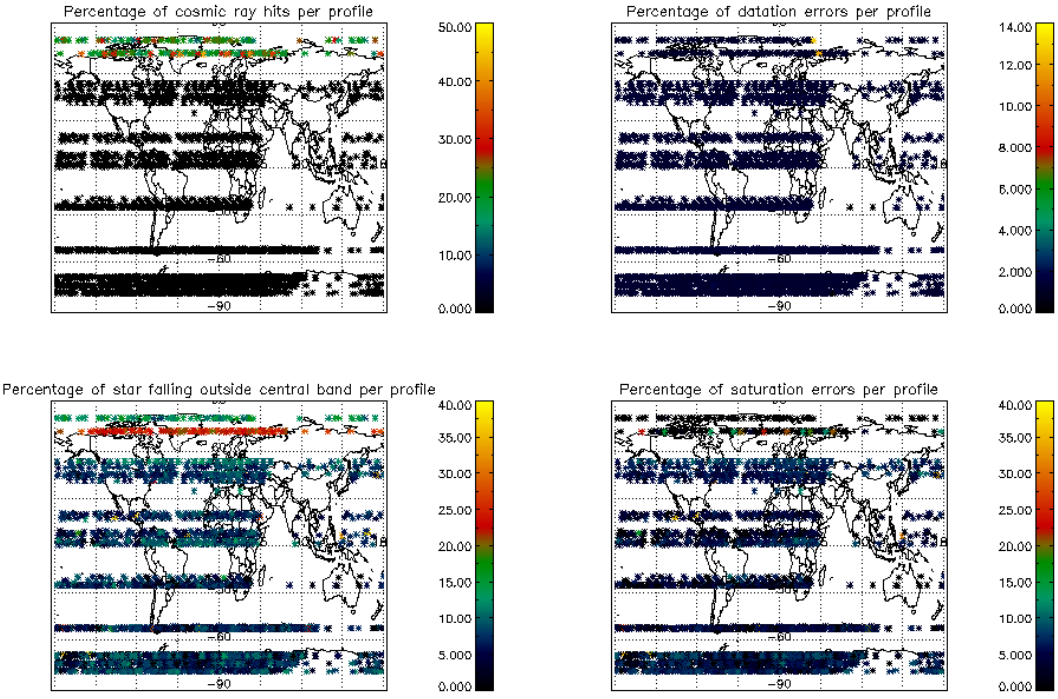

Figure 5.2-6: Level 1b product quality monitoring with respect to geo-location for DESCENDING ENVISAT passes

5.3 Spectral Performance

No spectral calibration exercises have been performed during the reporting period. In previous exercises the results exceeded the warning value which is 0.07 nm (fig. 5.3-1).

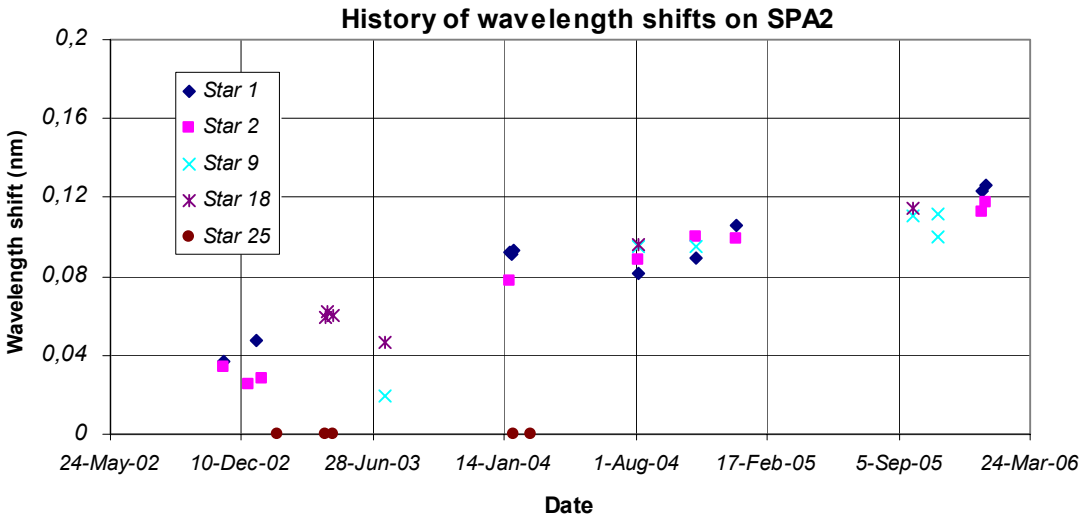

Figure 5.3-1: Wavelength shifts on SPA2 since 12th November 2002 calculated using different stars

The values reported in the plot of fig. 5.3-1 are, for every star ID (1, 2, 9, 18, 25), the spectral shift on SPA2 CCD for which a maximum correlation has been found between the reference spectrum and the one of the occultation.

During the last wavelength calibration analysis performed using two occultations of star 1 and two occultations of star 2 on 11th and 16th January 2006, the spectral shifts were greater than 0.07 nm (warning value). The QWG has decided to recalibrate the wavelength assignment when the new processor is ready.

5.4 Radiometric Performance

5.4.1 RADIOMETRIC SENSITIVITY

The monitoring performed consists of the calculation of the radiometric sensitivity of each CCD by computing the ratio between parts of the reference spectrum using specific stars (fig. 5.4-1). The parts of the spectrum used are:

- UV: 250–300 nm
- Yellow: 500–550 nm
- Red: 640–690 nm
- Ir1: 761-770 nm
- Ir2: 935-944 nm

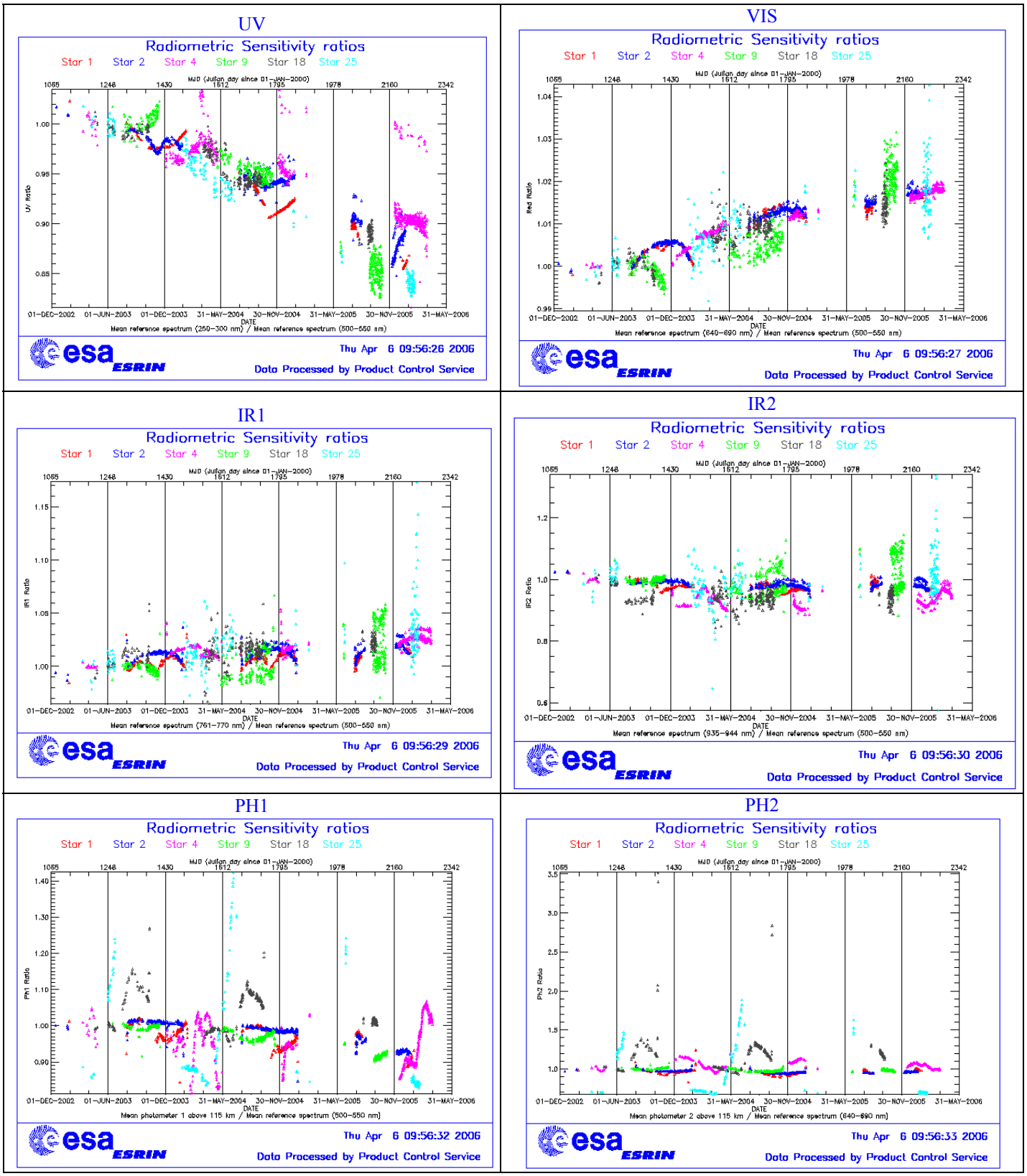

Figure 5.4-1: Radiometric sensitivity ratios since December 2002

For the spectrometers the ratios are with respect to the 'yellow' spectral range. For the photometers, the ratios are calculated by dividing the mean photometer signal above the atmosphere (115 km) by the 'yellow' spectral range (for PH1) or by the 'red' spectral range (for PH2).

The variation of the ratio should be within a given threshold which is set to 10% (see table 5.4-1 that corresponds to fig. 5.4-1). For every star, this variation is calculated as the difference between the maximum (or minimum) ratio, and the mean over the 15 first values (if there were not 15 values computed yet, all values would be used).

Table 5.4-1: Variation of RS for the different ratios (corresponds to fig. 5.4-1). Should be less than 10%

Star Id	% Variation of UV ratio	% Variation of Red ratio	% Variation of IR1 ratio	% Variation of IR2 ratio	% Variation of Ph1 ratio	% Variation of Ph2 ratio
1	3.15076	0.605267	0.401701	0.250543	8.55029	30.1656
2	0.810235	0.850594	0.625175	0.383392	8.27717	7.93166
4	0.460608	1.25498	1.52463	1.30163	8.08780	23.5227
9	13.0014	1.05504	0.783493	0.528085	5.59734	9.05862
18	1.73015	0.919592	0.844914	0.852089	14.7885	299.989
25	23.9743	1.35252	1.85261	1.35782	28.0870	147.396

For star 9 and 25 the UV ratio is greater than the threshold 10%. It is clear (fig. 5.4-1) that there is a global decrease of UV ratios for all the stars. This confirms the expected degradation suffered by the UV optics that is, anyway, very small considering also the small variation for the rest of the stars (table 5.4-1).

By looking at the photometers radiometric sensitivity ratios of fig. 5.4-1, it can be seen that every star has a variation that seems to be annual. The variation is significant for stars 25 and 18. After some investigations performed by the QWG that exclude an inaccurate reflectivity correction LUT or the different limbs (dark, twilight, bright) as sources of the variation, it has been concluded that the problem is not linked to the photometers. A further indication that the problem is not on the photometer sensitivity is that every star has a very different behaviour.

5.4.2 PIXEL RESPONSE NON UNIFORMITY

No new PRNU calibration has been performed during the reporting period. This means that the PRNU maps inside the ADF remain as they are without any change for the moment.

5.5 Other Calibration Results

Future reports will address other calibration results, when available.

6 LEVEL 2 PRODUCT QUALITY MONITORING

6.1 Processor Configuration

6.1.1 VERSION

Level 2 products from the operational ground segment have been disseminated during March 2006 to the users. About 70% of GOM_NL__2P products have been received by the DPQC team for routine quality control and long term trend monitoring. The current level 2-processor software version for the operational ground segment is GOMOS/4.02 (see table 6.1-1). The product specification is PO-RS-MDA-GS2009_10_3H. Users are also supplied with 2002-2005 data sets reprocessed by the last prototype processor GOPR_6.0c_6.0f developed and operated by ACRI. The next GOMOS operational ground segment version (GOMOS/5.00) will be in line with the prototype version used for this second reprocessing.

Table 6.1-1: PDS level 2 product version and main modifications implemented

Date	Version	Description of changes
23-MAR-2003	Level 2 version 4.02 at PDHS-E and PDHS-K	Algorithm baseline level 2 DPM 5.5: Section 3 • Add references to technical notes on Tikhonov regularization • Change High level breakdown of modules: SMO/PFG • Change parameter: NFS in l2 ADF • Change parameter σ_G in l2 ADF (Table 3.4.1.1-II) • Change content of Level 2/res products – GAP • Change time sampling discretisation • Add covariance matrix explanation Section 5 • Replace SMO by PFG VER-1/2: Depending on NFS, Apply either a Gaussian filter or a Tikhonov regularization to the vertical inversion matrix • Unit conversion applied on kernel matrix • Suppress VER-3 Section 6 • GOMOS Atmospheric Profile (GAP): not used in this version • Time sampling in equation (6.5.3.7-73)

31-MAY-2003	Level 2 version 4.00 at PDHS-E and PDHS-K	Algorithm baseline level 2 DPM 5.4: • Revision of some default values • Add a new parameter • Transmission model computation: suppress tests on valid pixels and species • Apply a Gaussian filter to the vertical inversion matrix • Very low signal values are substituted by threshold value
21-NOV-2002	Level 2 version 3.61 at PDHS-E and PDHS-K	Algorithm baseline level 2 DPM 5.3a: • Revision of some default values • Wording of test T11 • Dilution term computation of jend • Covariance computation scaling applied before and after

Table 6.1-2: GOPR level 2 product version and main modifications implemented

Date	Version	Description of changes
14-OCT-2005	GOPR_6.0f	• The optimisation of the DOAS iterations • Negative column densities and local densities not flagged anymore • Suppress the setting of maximum error in case of negative local densities • Correction of HRTP discrepancies, and error estimates fixed Configuration for second reprocessing: • 2^{nd} order polynomial for aerosol • Air fixed to ECMWF (local density set to 0 in the L2 products) • Orphal cross-sections for O_3 • GOMOS cross-sections for other species • Covariance matrix terms linked to air set to 0 • Air and NO_2 additional errors set to 0
17-MAR-2004	GOPR 6.0a	• Rename Turbulence MDS into High Resolution Temperature MDS (HRTP) • Add vertical resolution per species in local densities MDS • Add Solar zenith angle at tangent point and at satellite level in geolocation ADS • Add "tangent point density from external model" in geolocation ADS • Suppress contribution of "tangent point density from external model" in "local air density from GOMOS atmospheric profile" in geolocation ADS
18-AUG-2003	GOPR 5.4d	• Tikhonov regularisation is implemented
18-MAR-2003	GOPR 5.4b	• Modification to implement the computation of Tmodel for spectrometer B (in version 5.4b, the Tmodel for SPB is still set to 1)
30-JAN-2003	GOPR 5.4a	• Modifications for ACRI internal use only. No impact on level 2 products.

6.1.2 AUXILIARY DATA FILES (ADF)

The ADF's files in table 6.1-3 and 6.1-4 are used by the PDS to process the data from level 1 to level 2. For every type of file, the validity runs from the start validity time until the start validity time of the following one, but if an ADF file has been disseminated after the start validity time, it is obvious that it will be used by the PDHS-E and PDHS-K PDS only after the dissemination time (this happens the majority of the time). Note that the files outlined in yellow are the set of auxiliary files used during the reporting period.

Table 6.1-3: Table of historic GOM_PR2_AX files used by PDS for level 2 products generation. The GOM_PR2_AX is a file containing the configuration parameters used for processing from level 1b to level 2 products

Used by PDS for Level 2 products generation in period	GOM_PR2_AX (GOMOS Processing level 2 configuration file)
01-MAR-2002 → 29-JUL-2002	**GOM_PR2_AXVIEC20020121_165624_20020101_000000_20200101_000000** • Pre-launch configuration
30-JUL-2002 → 02-SEP-2002	**GOM_PR2_AXVIEC20020729_083851_20020301_000000_20100101_000000** • Maximum value of chi2 before a warning flag is raised (set to 5) • Maximum number of iterations for the main loop (set to 1)
03-SEP-2002 → 12-NOV-2003	**GOM_PR2_AXVIEC20020902_151029_20020301_000000_20100101_000000** • Maximum value of chi2 before a warning flag is raised (set to 100)
13-NOV-2003 → 22-MAR-2004	**GOM_PR2_AXVIEC20021112_170458_20020301_000000_20100101_000000** • Smoothing mode • Hanning filter • Number of iterations • Spectral windows to suppress the O2 absorption in the high spectral range of SPA2
23-MAR-2004 *Note*: this file was used by the GOMOS/4.02 processors before the IECF dissemination. The dissemination was done on 25th March 2004	**GOM_PR2_AXVIEC20040316_145613_20020301_000000_20100101_000000** • Pressure at the top of the atmosphere • Number of GOMOS sources data (used in GAP) • Activation flag for GOMOS sources data (GAP) • Smoothing mode (after the spectral inversion) • Atmosphere thickness

Table 6.1-4: Table of historic GOM_CRS_AX files used by PDS for level 2 products generation. The GOM_CRS_AX is a file containing the cross sections used for processing from level 1b to level 2 products

Used by PDS for Level 2 products generation in period	GOM_CRS_AX (GOMOS Cross Sections file)
01-MAR-2002 → 08-MAR-2002	**GOM_CRS_AXVIEC20020121_164026_20020101_000000_20200101_000000** • Pre-launch configuration
09-MAR-2003 → 29-JUL-2002	**GOM_CRS_AXVIEC20020308_185417_20020101_000000_20200101_000000** • Corrected NUM_DSD in MPH - was 14 and is now 19 - and corrected spare DSD format by replacing last spare by carriage returns in file GOM_CRS_AXVIEC20020121_164026_20020101_000000_20200101_000000

30-JUL-2002 → 25-MAR-2004	**GOM_CRS_AXVIEC20020729_082931_20020301_000000_20100101_000000** • O3 cross-sections summary description (SPA) • NO3 cross-sections summary description • O2 transmissions summary description • H2O transmissions summary description • O3 cross sections (SPA)
26-MAR-2004 *Note*: the file was disseminated on 27 Jan 2004 but could not be used by PDS until version GOMOS/4.02 was in operation	**GOM_CRS_AXVIEC20040127_150241_20020301_000000_20100101_000000** • Update of the O2 and H2O transmissions (S.A input) • Extension by continuity of the O3 cross-section for SPB

6.1.3 RE-PROCESSING STATUS

The improvement of the GOMOS processing chain is a continuous on-going activity, not only for the processing algorithm but also for the instrument characterization data. In order to provide the best quality products to the users and due to the normal delay between algorithm specification and implementation in the operational PDS, it has been decided to reprocess the GOMOS data using the GOPR prototype.

The first part of the second reprocessing activity covering years 2002- 2005 (using the prototype GOPR_6.0c_6.0f) is completed. Remaining gaps will be filled in early 2006. All reprocessed data can be retrieved via web query from http://www.enviport.org/gomos/index.jsp. FTP access to bulk reprocessing results (one tar file of GOMOS products per day) is allowed from the D-PAC: ftp://gomo2usr@ftp-ops.de.envisat.esa.int. See more details and latest status on http://www.enviport.org/boards/board_gomos.htm

The configuration of the prototype GOPR_6.0c_6.0f version is as follows:

Level 1b configuration:

- FP unfolding algorithm corrected
- Background correction of SPB in full dark limb
- Correction of the flat-field correction implementation
- Corrected reflectivity LUT
- Updated wavelength assignment
- Correction of the star spectra from reflectivity variations

Level 2configuration:

- DOAS iteration is based on the relative variation of NO_2 and NO_3 and no more χ^2.
- Suppress flagging of negative column densities
- Suppress flagging of negative local densities
- Suppress the setting to max-error in case of negative local densities
- Correction of the HRTP algorithm
- Aerosol polynomial degree 2
- Air fixed to ECMWF
- ORPHAL cross-sections only for O_3
- Air local density set to 0

- Error bar and vertical resolution for air set to 0
- Covariance matrix terms linked to air set to 0
- Air and NO_2 additional errors set to 0

6.1.3.1 O_2 density against ECMWF

We compare here the vertical profiles of the average difference between O_2 values retrieved from GOMOS and O_2 values inferred from ECMWF air data. The median, the mean and the 84 and 16 percentile limits of the distribution of the relative difference at each altitude level is computed. The results for GOMOS data for several datasets processed with GOPR version 6.0ab (first reprocessing) and with GOPR version 6.0cf (second reprocessing) are compared. Fig. 6.1-1 to fig. 6.1-3 present the values of the relative difference of O_2 concentration from GOMOS and from ECMWF: $(O_{2,GOMOS}-O_{2,ECMWF})/O_{2,ECMWF}$ in %, as a function of the vertical altitude for several datasets processed with the GOPR version 6.0cf. Only the non-flagged values of the GOMOS profiles measured in full dark limb are included. Also plotted are the vertical profiles of the median, the mean, and the 84 and 16 percentile limits of the difference. Besides the large dispersion of the values of the difference, one can note that the values of the mean profile of the difference are mostly negative, with large negative values around 60km-80km (depending on datasets, and with the exception of the bottom part of the profile for the dataset 3, fig. 6.1-3).

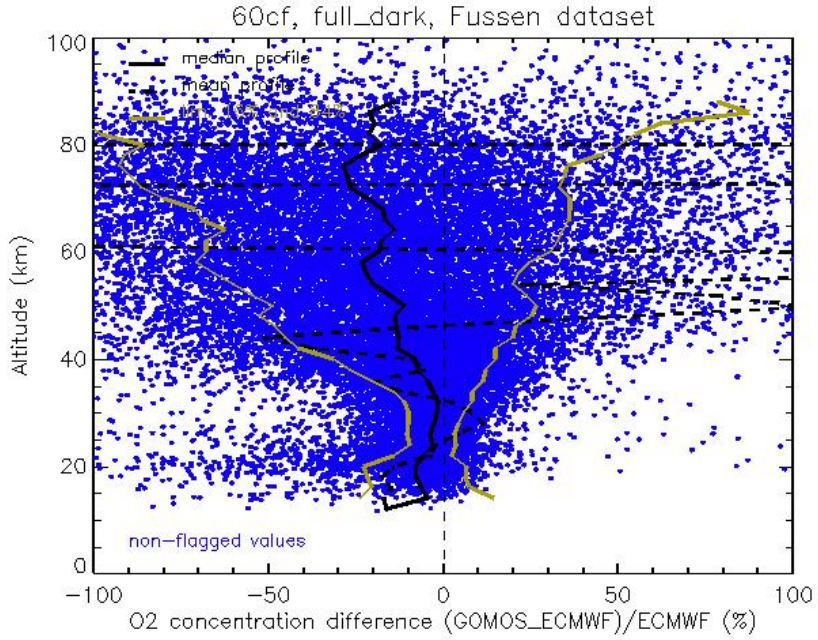

Figure 6.1-1: Relative difference of O_2 concentration from GOMOS measurements and from ECMWF data $(O_{2,GOMOS}-O_{2,ECMWF})/O_{2,ECMWF}$ in % as a function of vertical altitude (blue dots); vertical profile of the median of the difference (black solid line); vertical profile of the mean of the difference (black dashed line); 84 and 16 percentile limits (yellow solid lines). Only non-flagged values are included. Results are based on a dataset of 589 dark limb occultations at various latitudes (dataset 1) processed with GOPR version 6.0cf

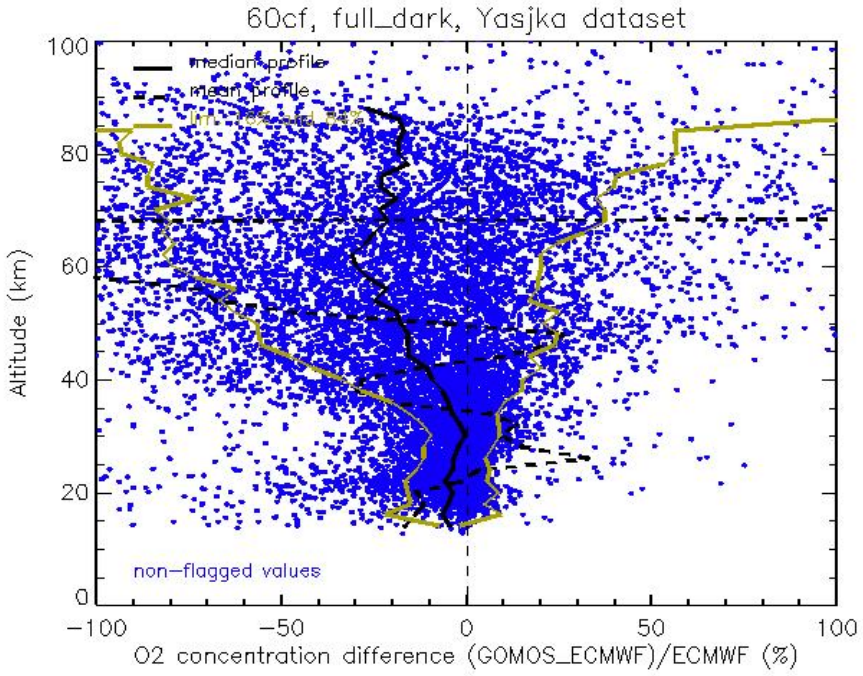

Figure 6.1-2: Same as fig. 6.1-1 for a dataset of 241 occultations measured in full dark limb at various latitudes (dataset 2)

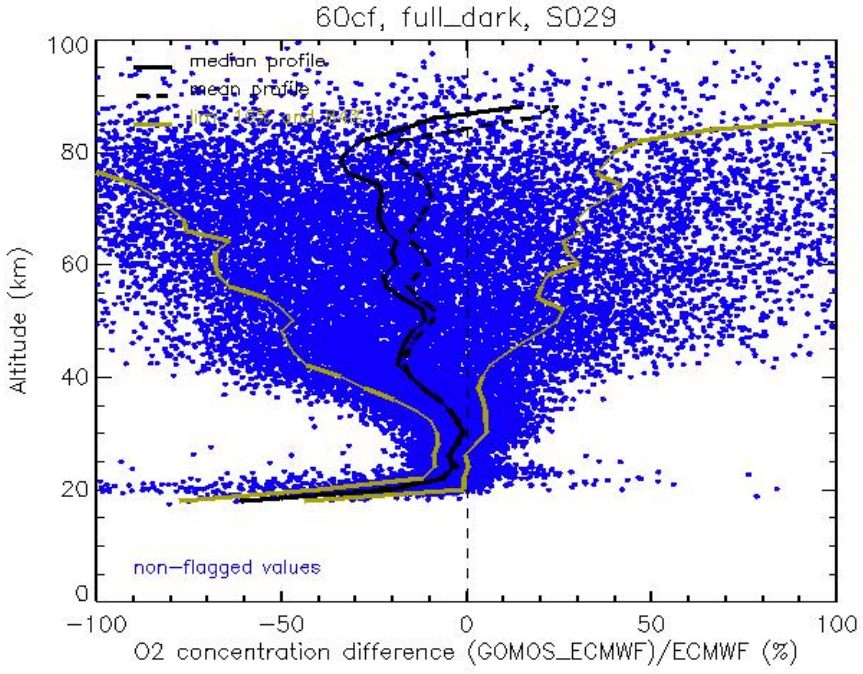

Figure 6.1-3: Same as fig. 6.1-1 for a dataset of 567 occultations measured in full dark limb at low latitudes (dataset 3)

The results from the two GOPR versions 6.0cf (2nd reprocessing) and 6.0ab (1st reprocessing) are compared. Left plots of fig. 6.1-4, 6.1-5 and 6.1-6 show the vertical profiles of the median of the difference, and of the 84 and 16 percentile limits for the three same datasets as above processed with GOPR version 6.0cf. Right plots of the figures present the same quantities for the datasets processed with GOPR version 6.0ab. From these results, it is obvious that the amplitude of the median difference between O_2 concentrations values by GOMOS and by ECMWF is generally lower for datasets processed with the new GOPR version than for datasets processed with the old GOPR version. Only for the last dataset at altitude levels lower than 20km, O_2 concentration values by GOMOS seem to show better agreement with ECMWF when processed with the old GOPR version than with the new one.

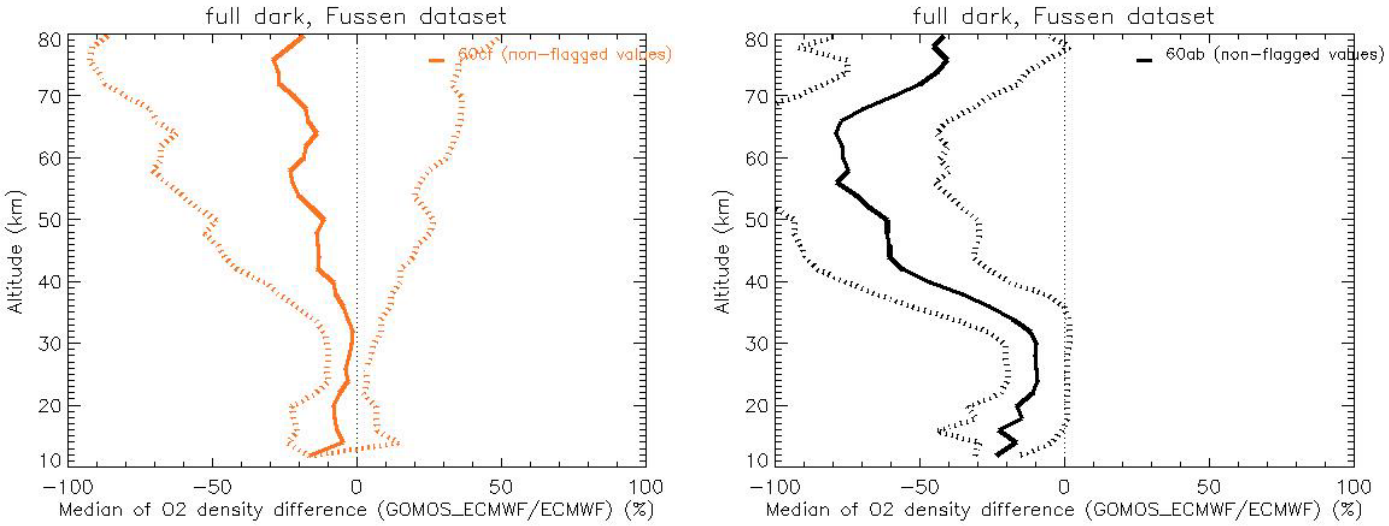

Figure 6.1-4: Vertical profiles of the mean difference between O_2 concentration values by GOMOS and by ECMWF: $(O_{2,GOMOS}-O_{2,ECMWF})/O_{2,ECMWF}$ in % (solid line); 84% and 16% percentile limits (dashed line). Results are based on a dataset of 589 dark limb occultations (only non-flagged values) at various latitudes (dataset 1) processed with GOPR 6.0cf (left) and GOPR 6.0ab (right)

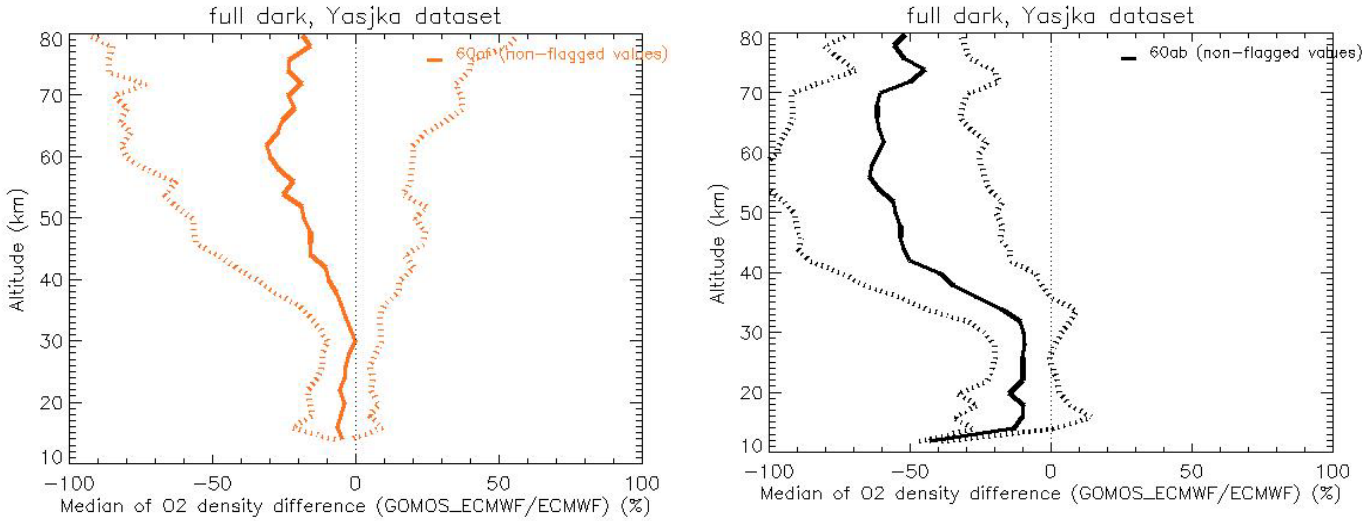

Figure 6.1-5: Same as fig. 6.1-4 for a dataset of 241 dark limb occultations at various latitudes (dataset 2) processed with GOPR 6.0cf (left) and GOPR 6.0ab (right)

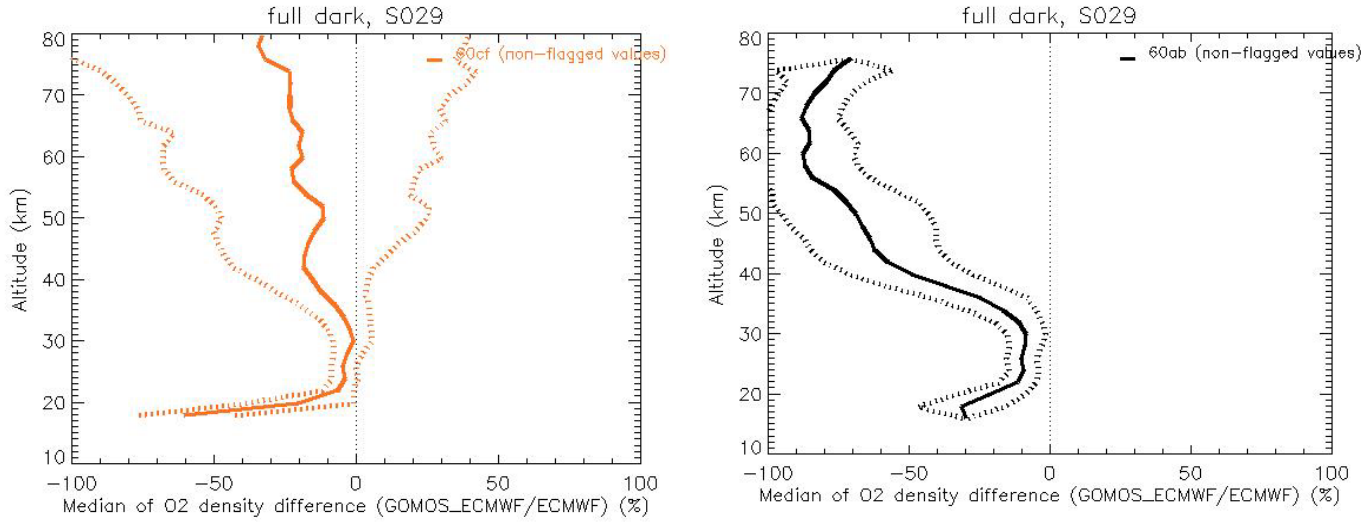

Figure 6.1-6: Same as fig. 6.1-4 for a dataset of 567 dark limb occultations at various latitudes (dataset 3) processed with GOPR 6.0cf (left) and GOPR 6.0ab (right)

The average values of the median difference for the two GOPR versions in a few km-thick altitude layers between 16km and 40km are given in table 6.1-5, 6.1-6 and 6.1-7. The limit values of the envelop calculated from the 84 and 16 percentile limits are also reported.

Table 6.1-5: Average value, envelop values from the 84 and the 16 percentile limits of the median difference between O_2 GOMOS and O_2 ECMWF by altitude layers, for dataset 1 processed with GOPR version 6.0ab (left columns) and processed with GOPR version 6.0cf (right columns). Only non-flagged values are included.

Dataset 1						
	GOPR version 6.0cf			GOPR version 6.0ab		
altitude layers	median	lim1	lim2	median	lim1	lim2
16km-20km	-7.3	-21.5	6.9	-17.7	-35.9	0.6
20km-24km	-5.6	-15.4	4.3	-12.0	-25.0	0.9
26km-30km	-2.7	-10.0	4.6	-9.6	-20.1	1.0
30km-34km	-2.1	-11.8	7.6	-12.9	-27.7	1.9
36km-40km	-6.6	-26.1	12.8	-35.7	-63.6	-7.9

Table 6.1-6: Same as table 6.1-5 for dataset 2

Dataset 2						
	GOPR version 6.0cf			GOPR version 6.0ab		
altitude layers	median	lim1	lim2	median	lim1	lim2

16km-20km	-5.0	-17.7	7.7	-11.4	-31.2	8.3
20km-24km	-4.3	-15.3	6.7	-11.6	-25.4	2.2
26km-30km	-1.9	-10.8	7.1	-9.6	-21.0	1.7
30km-34km	-1.7	-12.3	8.8	-12.6	-31.7	6.6
36km-40km	-6.9	-27.3	13.4	-33.4	-64.2	-2.7

Table 6.1-7: Same as table 6.1-5 for dataset 3

Dataset 3						
	GOPR version 6.0cf			**GOPR version 6.0ab**		
altitude layers	**median**	**lim1**	**lim2**	**median**	**lim1**	**lim2**
16km-20km	-40.4	-58.6	-22.2	-26.5	-40.4	-12.6
20km-24km	-10.1	-20.0	-0.2	-13.9	-22.1	-5.6
26km-30km	-2.8	-8.1	2.6	-9.0	-15.0	-3.0
30km-34km	-2.5	-10.3	5.4	-11.8	-20.9	-2.8
36km-40km	-11.5	-27.0	4.0	-36.6	-56.3	-16.9

The statistical comparison between O_2 local density values by GOMOS and by ECMWF data for three datasets of full dark occultations processed with GOPR version 6.0cf shows that in average, at all altitude levels up to 80km, O_2 local density values by GOMOS are lower than O_2 local density values inferred from ECMWF data. In this altitude range, for the three datasets investigated, the minimum amplitude of the average relative difference $(O_{2,GOMOS}-O_{2,ECMWF})/O_{2,ECMWF}$ is between 0 and -1% at 30km. Between 25km and 35km, it is estimated to be about –2% in average. These figures stress out a significant reduction of the discrepancy with ECMWF observed with GOPR version 6.0ab, for which larger negative values of the difference were calculated (about –10% in average between 25km and 35km; minimum amplitude between –8% and –9%).

6.2 Quality Flags Monitoring

In this section, some information contained in the Quality Summary data set of the level 2 products of March 2006 is shown. In particular, the percentage of flagged points per profile for the local species O_3, H_2O, NO_2 and Air is depicted. Only products in dark limb illumination conditions and without fatal errors (error flag in the MPH set to "0") are used.

A profile point in a level 2 product is flagged when:

- The local density is less than a given minimum value
- The local density is greater than a given maximum value
- A negative local density was found
- The line density is not valid. And it occurs when:
  - The acquisition from level 1b is not valid
  - There is no acquisition used for reference star spectrum

- The line density is less than a given minimum value
- The line density is greater than a given maximum value
- A negative line density was found

For species: air, aerosol, O_3, NO_2, NO_3, OClO

- No convergence after a given number of LMA iterations
- χ^2 out of LMA is bigger than χ^2
- Failure of inversion

For species: O_2, H_2O

- Spectro B only: no convergence
- Spectro B only: data not available
- Spectro B only: covariance not available

There are points mainly between -45° and +35° latitude because in this period of the year full dark illumination condition occultations (only those products have been used for these plots) are found on that region. In summer, full dark illumination data are mainly in the Southern Hemisphere while in winter it is the contrary: full dark illumination occultations are found mainly in the Northern Hemisphere.

Looking at fig. 6.2-1, the most evident characteristic that can be observed is the high percentage of flagged points per profile for H_2O. Users should not use these data, as their quality is still poor. The percentage of flagged points per profile for O_3 and Air is around 35% whereas for NO_2 it becomes 60%. It can be seen also that there are latitudinal bands with almost the same color (same percentages). This means that the percentages of flagged points per profile have a dependence on the stars that have been observed: a given star is always observed at the same latitude but at different longitude.

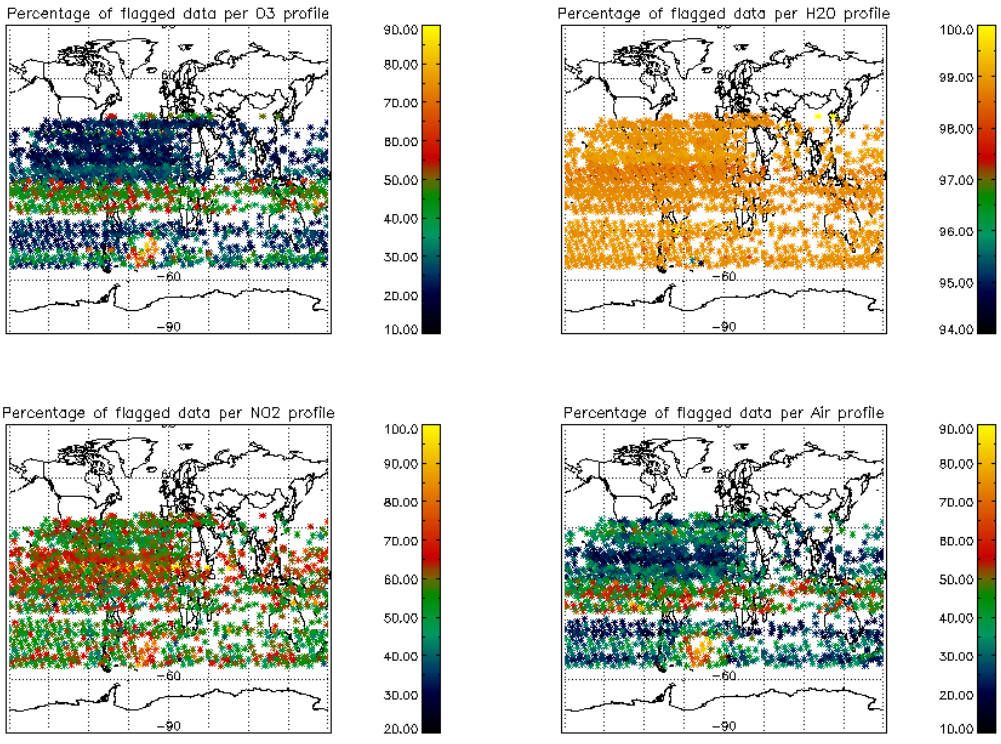

Figure 6.2-1: Percentage of flagged points per profile

Fig. 6.2-2 shows the same information as in fig. 6.2-1 but for given species **valid altitude ranges** (see table 6.2-1), that is, altitude ranges where data with the best quality should be found. If there are no points within the altitude range for a given occultation then a value of -20 is used. For O_3 the percentage of flagged points per profile is on average around 10% between 20 and 60 Km altitude. For NO_2 it becomes 20 % for altitudes between 20 and 50 Km and for Air profiles, the percentage of flagged points is around 15% for altitudes between 25 and 45 Km. For H_2O, considering the whole profiles or considering points below 50 Km does not change the high percentage of flagged points.

Table 6.2-1: Species valid altitude ranges

Specie	O_3	NO_2	Air	H_2O
Valid altitude range (km)	20 - 60	20 - 50	25 - 45	< 50

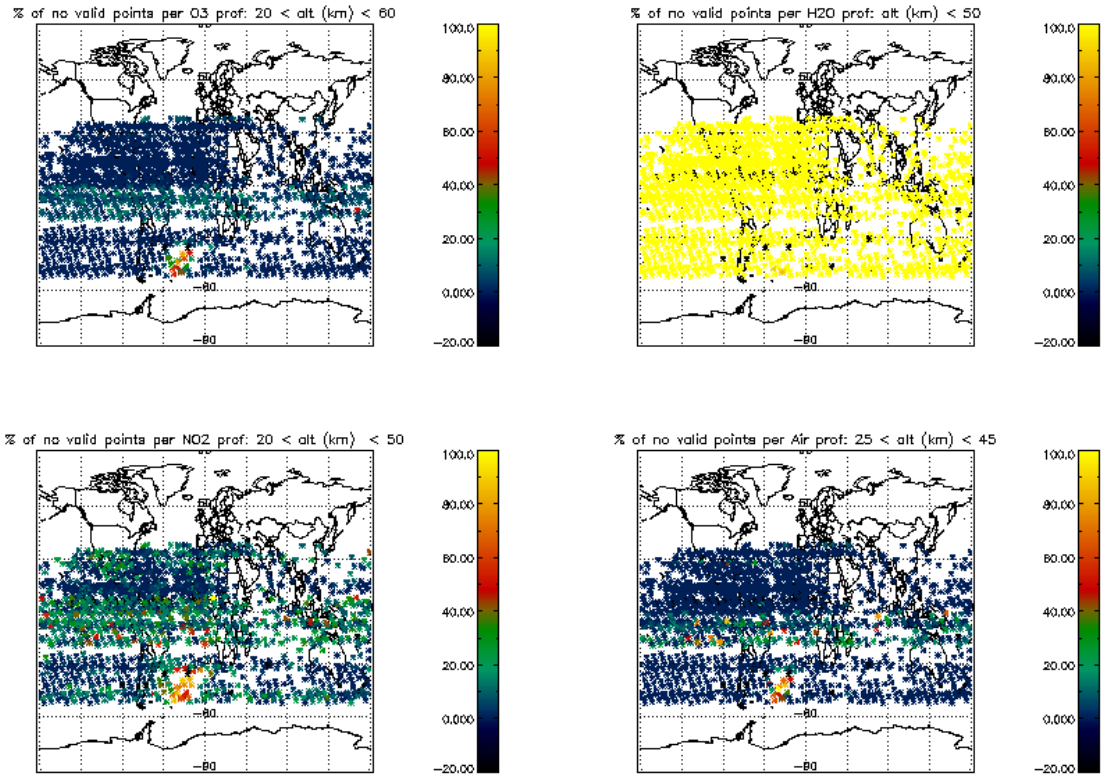

Figure 6.2-2: Same as fig. 6.2-1 but for valid altitude ranges of table 6.2-1

6.3 Other Level 2 Performance Issues

The plot presented in fig. 6.3-1 is the average of the Ozone values during March 2006 in a grid of 0.5 degrees in latitude per 1 km in altitude. Only occultations in dark limb have been used. Even though there is a reduction on latitude coverage due to the restricted azimuth field of view of the instrument, still some known characteristics can be seen:

- O_3 concentrations show a decrease with latitude near 40 km altitude. In the lower latitudes O_3 is generated by photolysis of O_2
- In the middle stratosphere (25-30 km) O_3 is strongly influenced by transport effects. Strong meridional and zonal transport is visible in middle and higher latitudes
- The lower stratosphere shows an O_3 increase with latitude. Highest values can be found within higher latitude regions due to downward transport of rich air masses

However, other characteristics seem not to be realistic as some high values at –45 degrees latitude at high altitude (issues to be probably related to the South Atlantic Anomaly).

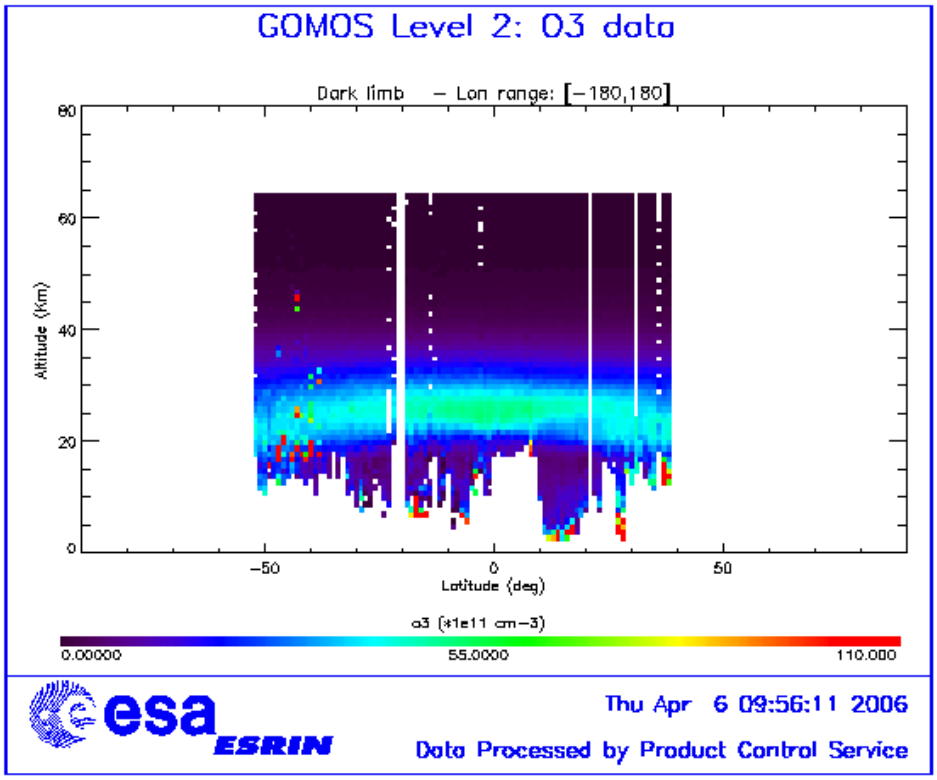

Figure 6.3-1: Average GOMOS O_3 profile during the reporting month: average in a grid of 0.5° latitude x 1 km altitude

7 VALIDATION ACTIVITIES AND RESULTS

7.1 GOMOS-ECMWF Comparisons

7.1.1 TEMPERATURE AND OZONE COMPARISONS

Due to restrictions in the current METEO product format, filtering of METEO data is not possible. ECMWF results are therefore partially based on data that are not to be used for scientific application, as mentioned in the disclaimer (http://envisat.esa.int/dataproducts/availability/disclaimers)

Find below the summary of ECMWF GOMOS monthly report for March 2006 data:

- Good agreement was found between GOMOS and ECMWF temperatures.
- GOMOS temperatures were lower than ECMWF temperatures in most of the stratosphere and mesosphere, but area mean departures were less than 1% in most of the stratosphere, up to 1hPa. Slightly larger departures (between -1 and -2%) were found above 1hPa.
- Large differences were found between GOMOS and ECMWF ozone values (over 50% in places).
- Large scatter of GOMOS ozone data.
- No water vapour data in NRT GOMOS BUFR files.
- The monitoring statistics for March were produced with the operational ECMWF model, CY30R1.

The full March 2006 ECMWF report can be found in the link below:
http://earth.esa.int/pcs/envisat/tmp_calval_res/2006/ecmwf_gomos_monthly_200603_all.pdf

7.2 GOMOS-Climatology comparisons

Results are presented when available.

7.3 GOMOS Assimilation

Results are presented when available.

7.4 Consistency Verification: GOMOS-GOMOS Inter-comparison

Results are presented when available.

7.5 Inter-Comparison with external data

Results are presented when available.